Neogene uplift of central eastern Patagonia: Dynamic response to active spreading ridge subduction

Benjamin Guillaume, Joseph Martinod, Laurent Husson, Martin Roddaz, Rodrigo Riquelme

Neogene uplift of central eastern Patagonia: Dynamic response to active spreading ridge subduction?

Benjamin Guillaume,[1,2,3,4] Joseph Martinod,[1,2,3] Laurent Husson,[5] Martin Roddaz,[1,2,3] and Rodrigo Riquelme[6]

Received 2 May 2008; revised 8 October 2008; accepted 23 December 2008; published 10 April 2009.

[1] The Chile Triple Junction (CTJ) episodically migrated northward during the past 14 Ma from 54°S to its present-day position at 46°30′S, as different almost trench-parallel spreading segments entered in subduction. This migration resulted in the opening of an asthenospheric window below Patagonia, inducing a disturbance in the regional mantle convection. On the overriding plate, the middle Miocene time corresponds to a major change in the central Patagonian basin dynamics, with a transition from subsidence to generalized uplift. The detailed mapping and the morphological study of post-middle Miocene terraces evidence regional-scale trench-parallel tilt histories that differ depending on latitude. South of 46°30′S, the slopes of the fluvial terraces indicate a change from northward to southward tilt during late Miocene. Terraces younger than the early Pliocene do not show any trench-parallel tilt. North of 46°30′S, in contrast, only northward tilt, active until the Pleistocene, is recorded. We use a semianalytical model of dynamic topography which suggests that the northward migration of the Chile Triple Junction should be accompanied by a dynamic uplift of the central Patagonian basin. Uplift would cause both north directed and south directed tilt, north and south of the triple junction, respectively, with values of ∼0.1–0.2% 500 km east of the trench. Tilt measured in the southeastern part of the central Patagonian basin (∼0.1%) is comparable to values predicted using the semianalytical model. The dynamic topography associated to the Chile ridge subduction may have exerted a major control on the Neogene dynamics of Patagonia. **Citation:** Guillaume, B., J. Martinod, L. Husson, M. Roddaz, and R. Riquelme (2009), Neogene uplift of central eastern Patagonia: Dynamic response to active spreading ridge subduction?, *Tectonics*, *28*, TC2009, doi:10.1029/2008TC002324.

1. Introduction

[2] Geologists often consider that the topography of the Earth essentially results from isostasy, topographic highs being balanced by crustal roots and/or hot lithospheric mantle [*Airy*, 1855; *Pratt*, 1859; *Froidevaux and Isacks*, 1984; *Molnar et al.*, 1993; *Garzione et al.*, 2006]. Mantle dynamics, however, also induce forces that deflect the Earth topography. Global numerical models predict associated vertical displacements of several hundreds of meters [*Hager and Clayton*, 1989; *Ricard et al.*, 1993; *Le Stunff and Ricard*, 1997; *Čadek and Fleitout*, 2003] and, therefore, that the direct contribution of mantle dynamics in the topography of the Earth is far from being negligible. Dynamic topography reaches its maximum amplitude above subduction zones, where mass anomalies are large at depth [e.g., *Mitrovica et al.*, 1989; *Gurnis*, 1993; *Zhong and Gurnis*, 1994; *Husson*, 2006].

[3] In continental domains, the dynamic component of topography is difficult to discriminate because the altitude is largely controlled by lithospheric loads and composition, which are highly variable. Active continental margins are nevertheless affected by long-wavelength surface deflections, and changes in the dynamics of subduction should be accompanied by vertical movements that can be recorded by the geological imprint [*Mitrovica et al.*, 1989; *Mitrovica et al.*, 1996; *Catuneanu et al.*, 1997; *Pysklywec and Mitrovica*, 2000; *Lock et al.*, 2006]. For instance, *Mitrovica et al.* [1989] showed that the process of subduction beneath western North America during the Cretaceous resulted in large-scale vertical deflection and tilting of the continental lithosphere that was followed by a Tertiary uplift of the area.

[4] In this paper, we study the Neogene evolution of central Patagonian, which was uplifted following the subduction of the Chile Ridge below the Andes since the middle Miocene. We focus our study on the mild deformed central Patagonian basin (Figure 1), which extends in the W-E direction from the eastern foothills of the Patagonian Andes to the Atlantic coast and in the N-S direction from the Sierra San Bernardo to the Deseado massif because this area is poorly affected by post-middle Miocene tectonics. Moreover, this region remained ice-free during glaciations. It shows a pristine morphology preserved from the erasure of glaciers that will be used to evidence its long-term Neogene uplift. The central Patagonian basin, which almost overlays the inland part of the San Jorge Gulf basin

[1]LMTG, Université de Toulouse, UPS (OMP), Toulouse, France.
[2]LMTG, CNRS, Toulouse, France.
[3]LMTG, IRD, Toulouse, France.
[4]Now at Dipartimento Scienze Geologiche, Università degli Studi Roma TRE, Rome, Italy.
[5]Géosciences Rennes, UMR 6118, Université Rennes-1, CNRS, Rennes, France.
[6]Departamento de Ciencias Geológicas, Universidad Católica del Norte, Antofagasta, Chile.

0278-7407/09/2008TC002324

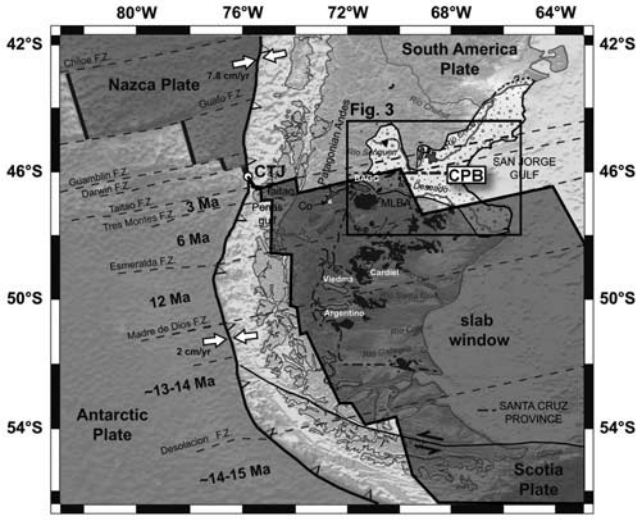

Figure 1. Geodynamic setting of southern South America displaying the different active segments and transform fault zones (FZ) of the Chile Ridge (modified from *Cande and Leslie* [1986]). Timing of ridge subduction is indicated by bold black numbers [from *Gorring et al.*, 1997] and relative present-day convergence velocities [from *De Mets et al.*, 1994]. The Chile Triple Junction (CTJ) is currently located west of the Taitao Peninsula. Neogene plateau basalts, including the Meseta del Lago Buenos Aires (MLBA), are displayed in black [from *Panza et al.*, 2003] and slab window current projection at the surface in gray [from *Breitsprecher and Thorkelson*, 2008]. The central Patagonian basin (CPB) and the Cosmelli basin (Co), south of the Buenos Aires–General Carrera Lake (BAGC), are displayed in white. The location of Figure 3 is indicated by the black box.

[*Bianchi*, 1981], is located at the latitude of the present-day Chile Triple Junction (CTJ), where the Chile active spreading ridge subducts beneath South America.

[5] During the past 14 Ma, the CTJ migrated northward, from the latitude of 54°S to its present-day position at about 46°30′S, west of the Taitao Peninsula, as different segments of the Chile spreading ridge successively entered the subduction zone [*Cande and Leslie*, 1986]. North of the CTJ, the convergence rate between Nazca and South American plates is 7.8 cm a^{-1}, whereas south of the CTJ, the convergence rate between South America and the Antarctic oceanic plate decreases to 2 cm a^{-1} [*De Mets et al.*, 1994], leading to the opening of an asthenospheric window [*Ramos and Kay*, 1992; *Kay et al.*, 1993; *Gorring et al.*, 1997, 2003; *D'Orazio et al.*, 2000, 2001, 2003, 2005; *Gorring and Kay*, 2001; *Guivel et al.*, 2003, 2006; *Lagabrielle et al.*, 2004, 2007; *Espinoza et al.*, 2005; *Breitsprecher and Thorkelson*, 2008] that disturbs mantle dynamics beneath the continent (Figure 1). In order to investigate the impact of the associated mantle flow on the vertical surface motion, we synthesize published data and analyze the evolution of sedimentation, erosion, and tectonic features as well as evidence of deformation during the Neogene. We produce a regional-scale map of the post-middle Miocene system of terraces, and measure the tilting affecting each of the terraces to characterize the uplift of the central Patagonian basin. Then, we compare its evolution with a semianalytical model of dynamic topography simulating the geodynamic context of Patagonia.

2. Geological Setting of Central Patagonia

2.1. Late Oligocene to Early Middle Miocene: Marine Transgression and Synorogenic Continental Molasse

[6] From late Oligocene to early Miocene, a widespread transgression occurred in the Patagonian basin. This transgression is marked by the deposition of nearshore marine Centinela Formation and lateral equivalents (Figure 2). The "Patagonian transgression" covered most of southern Patagonia [*Malumián*, 1999]. The epicontinental seaway was largely open to the south, south of the Deseado massif, and to the east, north of the Deseado massif [*Malumián*, 1999]. Close to the present-day Atlantic coast, the corresponding marine series are the Chenque (San Jorge Gulf) and Monte León formations. In Chile, marine series corresponding to the Centinela Formation are assigned to the Guadal Formation [*Suárez et al.*, 2000; *De la Cruz and Suárez*, 2006]. The marine transgression extended to the west above part of the present-day Cordillera, and Oligo-Miocene marine sediments are preserved in the Cosmelli syncline [*Flint et al.*, 1994; *De la Cruz and Suárez*, 2006], south of the Buenos Aires–General Carrera Lake. Although this locality is only 100 km east of the Miocene outcrops of the Penas Gulf area on the Pacific coast (Figure 1), the different macroinvertebrate fauna suggest that the marine transgression that invaded Patagonia from the Atlantic to the Guadal area was separated from the Pacific Ocean by the continuous geographic barrier of the Andean Cordillera [*Frassinetti and Covacevich*, 1999; *Flynn et al.*, 2002]. Marine series form an Oligocene to early Miocene eastward prograding sequence of coarse conglomerates, sandstones, and shales containing shells and microfossils [*Ramos*, 1989; *Barreda and Caccavari*, 1992; *Bellosi and Barreda*, 1993; *Frassinetti and Covacevich*, 1999; *Malumián*, 1999]. The thickness of the deposits reaches 500 m on the Atlantic coast [*Bellosi and Barreda*, 1993]. It generally varies between 225 and 375 m in the Cordillera foothills [*Ramos*, 1989], and in the Cosmelli syncline, measured thicknesses range between 110 m [*De la Cruz and Suárez*, 2006] and 650 m [*Flynn et al.*, 2002].

[7] South of the CTJ, marine series are followed by fluvial deposits of the Santa Cruz Formation and its lateral equivalent (Río Zeballos Group) [*Ramos*, 1989; *Suárez et al.*, 2000; *De la Cruz and Suárez*, 2006] (Figure 2). This synorogenic formation consists of sandstones and silts, interbedded with conglomerate lenses that deposited in a high-energy fluvial environment [*Ramos*, 1989; *De la Cruz and Suárez*, 2006]. The Santa Cruz Formation thickness locally reaches up to 1500 m, south of Buenos Aires–General Carrera Lake [*Ramos*, 1989] and exhibits minimum thicknesses of 900–1000 m in the Cosmelli basin [*De la Cruz and Suárez*, 2006]. These deposits have been dated using intercalated tuffs levels between 22 and 14 Ma [*Blisniuk et al.*, 2005]. North of the CTJ, the Río Frias Formation and lateral

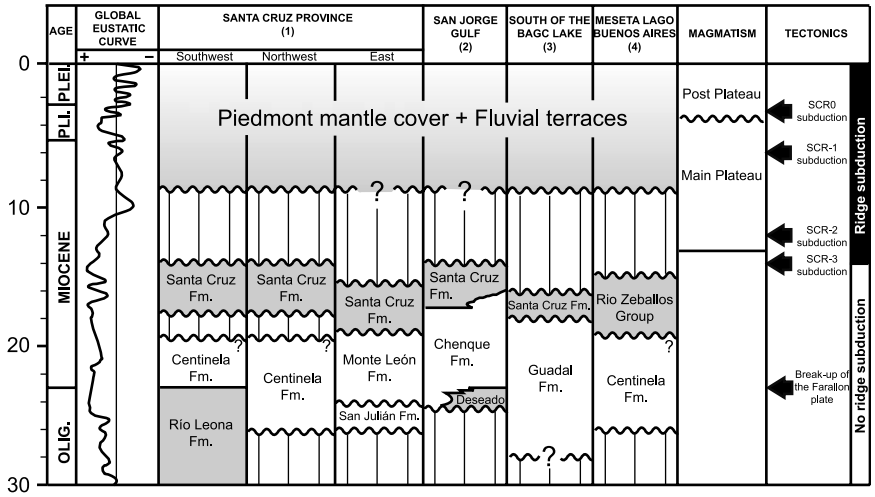

Figure 2. Chronological table displaying the stratigraphy of (1) the southwestern, northwestern and eastern sectors of the Santa Cruz province [*Parras et al.*, 2008], (2) the San Jorge Gulf [*Malumián*, 1999], (3) the south of the Buenos Aires–General Carrera (BAGC) Lake [*De la Cruz and Suárez*, 2006], and (4) the Meseta del Lago Buenos Aires [*Lagabrielle et al.*, 2007]. Continental formations are gray, and marine formations are white. The main magmatic and tectonic events along with the global eustatic curve [*Haq et al.*, 1987] are also indicated.

equivalents (Río Mayo and Pedregoso formations) also correspond to fluvial series that were deposited during the middle Miocene [*Marshall and Salinas*, 1990]. The maximum outcropping thickness of the Río Frias formation is about 250 m. Contractional tectonics during deposition of the continental series are evidenced by synsedimentary structures. Growth folds and intraformational thrusts have been reported in Chile in the Cosmelli syncline and south of the region of Río Las Horquetas and Meseta del Guenguel [*Flint et al.*, 1994; *Suárez and De la Cruz*, 2000; *Lagabrielle et al.*, 2004].

[8] The Patagonian transgression and the deposition of the overlying continental series are the result of a major change in the Andean geodynamic context. At around 26 Ma, the Farallon plate broke up [*Lonsdale*, 2005]. This period is also marked by a change to a more trench-perpendicular and faster convergence between the oceanic and South American plates [*Pardo-Casas and Molnar*, 1987; *Somoza*, 1998; *Lonsdale*, 2005]. Fission track analyses evidence an acceleration of the denudation at the western margin of the Cordillera during the late Oligocene [*Thomson et al.*, 2001], coeval with the deposition of the Oligo-Miocene series. Then, Oligocene and Miocene series were deposited during a major contractional period of the Andes at the latitude of the central Patagonian basin [*Ramos*, 1989; *Lagabrielle et al.*, 2004]. Between 47°30′S and 49°S, this shortening resulted in the formation of a complex fold-and-thrust belt in which the Tertiary molasse sequence (marine and continental) is involved [*Ramos*, 1989]. Shortening varies between 45 and 22 km from the north (47°40′S) to the south (49°S) of the fold-and-thrust belt [*Ramos*, 1989] and is at least of 35 km during the late Miocene in the fold belt at 50°S [*Kraemer*, 1998]. The segment of the Patagonian Andes located north of the present-day triple junction is characterized by a weaker Oligo-Miocene shortening, resulting in restricted areas of foreland sedimentation that only accumulated about 100 m of synorogenic deposits [*Ramos and Kay*, 1992].

2.2. Late Miocene to Holocene: Back-Arc Plateau Basalts and Widespread Detrital Cover

[9] The Patagonian back-arc region has been the locus of widespread volcanic activity during the entire Cenozoic. South of 46°S, a magmatic pulse started ~13 Ma ago during middle Miocene [*Ramos and Kay*, 1992; *Gorring et al.*, 1997; *Guivel et al.*, 2006]. The late Miocene to Pleistocene magmatism mainly consists of massive tholeiitic plateau lavas covered by less voluminous alkalic postplateau lavas [*Gorring et al.*, 1997]. The emplacement of main plateau lavas has been dated between 12.4 and 3.3 Ma at the Meseta del Lago Buenos Aires and between 8.2 and 4.4 Ma at the Meseta Chile Chico [*Guivel et al.*, 2006]. South of 46°30′S, the main plateau lavas range between 12 and 7 Ma in the western part of the back-arc region and between 5 to 2 Ma in the eastern part of the Deseado massif [*Gorring et al.*, 1997]. The Plio-Pleistocene postplateau basalts have ages from 3.4 to 0.125 Ma [*Gorring et al.*, 2003] at the Meseta del Lago Buenos Aires. Therefore, most of the plateau and postplateau basalts postdate the deposition of the early to middle Miocene continental molasses, and their emplacement helps in dating the subsequent evolution of the region. In the region of Buenos Aires–General Carrera Lake, plateau basalts are emplaced on a planar surface gently tilted toward the east, and seal the eastern thrust front of the Patagonian Andes [*Ramos*, 1989; *Lagabrielle et al.*, 2004]. This implies that the compressive tectonic activity in this part of the orogen essentially ceased before 13 Ma [*Lagabrielle et*

al., 2007]. The same observation has been done by *Coutand et al.* [1999] at the latitude of Viedma lake (49°S), where gently tilted early Pliocene basalts [*Mercer et al.*, 1975] unconformably overlie deformed Paleogene sediments.

[10] In northern Patagonia, in contrast, transpression is still active. Oblique thrusting predominates outside the magmatic arc, and dextral strike-slip shear zones develop within it [e.g., *Lavenu and Cembrano*, 1999; *Cembrano et al.*, 2002]. The transpressional dextral Liquiñe-Ofqui fault, whose present-day activity is demonstrated by seismic records [*Lange et al.*, 2008], is a more than 900-km-long structure that initiates close to the current Chile Triple Junction.

[11] In central Patagonia, following the deposition of the Santa Cruz Formation, the depositional environment drastically changes. The Santa Cruz Formation is overlain by late Cenozoic continental deposits, as the so-called "Rodados Patagonicos," which have formerly been accurately described by *Feruglio* [1950]. These series correspond to poorly consolidated conglomerates that are widespread from the Andean foothills to the Atlantic coast and which thickness often does not exceed 10 m. The pebbles generally have a roughly constant size from the Andes to the Atlantic Ocean. They form a piedmont mantle cover in which the activity of fluvial systems elaborated a succession of fluvial terraces (Río Senguerr, Río Deseado, Cañadon Salado, Cañadon del Carril, Río Mayo) (see *Panza* [2002] for a review).

3. Post-Middle Miocene Landscape Evolution

[12] We mapped the conglomeratic surfaces, (piedmont mantle cover and fluvial terraces), on the basis of the synthesis of *Panza* [2002], complemented by 1:250,000 scale geological maps of the Servicio Geológico Minero Argentino [*Dal Molin et al.*, 1998; *Giacosa*, 1998; *Sciutto et al.*, 2000; *Cobos and Panza*, 2001; *Servicio Geológico Minero Argentino*, 2001; *Ardolino et al.*, 2003; *Escosteguy et al.*, 2003; *Sciutto et al.*, 2004; *Panza and Genini*, 2005] and observation of Landsat images and SRTM digital elevation model, analyses being confirmed by field observations (Figure 3). We will use the different surfaces as geologic markers to infer the geomorphologic and tectonic evolution since middle Miocene.

3.1. Description of Piedmont Mantle Cover and Fluvial Terrace Systems

[13] We distinguish three sectors in which piedmont mantle cover deposits have been preserved (Río Guenguel and Arroyo Verde areas to the west, and Pampa del Castillo area to the east), extending from the Andes foothills to the Atlantic coast (Figure 3). Piedmont mantle cover gently dips eastward and results from the coalescence of alluvial cones [*Panza*, 2002], that generally lie more or less conformably on the Santa Cruz continental formation (early to middle Miocene) in the western region, and on the marine Patagonia and Chenque formations (late Oligocene to early Miocene) close to the Atlantic Ocean. The higher surface is ~850 m above sea level (asl) in the Río Guenguel area and is still remarkably high close to the Atlantic coast (~750 m asl in Pampa del Castillo, only 25 km NW of the coast). Seven younger levels of piedmont surfaces (T2Gu to T8Gu, see Figure 3) are preserved in the Río Guenguel area. The difference in elevation between the first and last level is roughly 200 m.

[14] Fluvial terrace levels correspond to more recent systems of terraces resulting from the activity of rivers flowing from the Andes into the Atlantic Ocean. We distinguish three main groups of terraces corresponding to different fluvial systems: (1) the Cañadon Salado-Cañadon del Carril, (2) the Río Senguerr, and (3) the Río Deseado. These fluvial terraces result from the action of rivers whose flow has been incomparably larger than that of the present-day rivers going to the Atlantic Ocean. The semiarid climate of the continent, east of the Cordillera, and the fact that the present-day drainage divide between rivers flowing toward the Atlantic Ocean versus rivers flowing toward the Pacific Ocean is essentially located on the eastern and drier side of the mountain belt explains the modest flow of these rivers at present-day. In fact, the drainage divide shifted eastward after Neogene glaciations remodeled the Andean landscape. Between 45°S and 47°30′S, several major glacial valleys crosscut the chain, the most striking example being the valley occupied by the Buenos Aires–General Carrera Lake and the Río Baker. Their formation resulted in the capture of Andean rivers flowing eastward by the Pacific side, subsequently starving rivers flowing into the Atlantic Ocean. During cold periods, however, the ice cap covers the Patagonian Andes, fills valleys in the Cordillera and the eastward flowing drainage is reactivated [*Feruglio*, 1950; *Mercer*, 1976; *Turner et al.*, 2005]. This evolution of the watershed system explains the presence of several major fluvial terrace systems that do not correspond to the flow of the present-day rivers.

[15] The Cañadon Salado–Cañadon del Carril fluvial system, located southwest and south of the Río Senguerr system, is the oldest preserved fluvial system of the study area. The Cañadon Salado and Cañadon del Carril are currently temporary rivers flowing into the Río Senguerr (Figure 3). The second level of this fluvial system (T2Cs) covers the Ruta 16 valley, indicating that the paleoriver flowed out east of its present-day course before being captured by the paleo-Río Senguerr, that was flowing at that time in the arc-shaped Hermoso valley (Figure 4). The capture of the Cañadon Salado occurred before the emplacement of the T3Cs deposits since the latter displays the same spatial organization than the present-day river (Figure 4).

[16] The Río Senguerr is currently 395 km long, flowing from Fontana Lake at an elevation of 925 m asl, into the Musters and Colhué-Huapi lakes at an elevation of 270 m asl. Its main tributaries are the Arroyo Verde and the Río Mayo. It produced a system of eight terraces, exposed from Nueva Lubecka to the north to the abandoned Hermoso valley. The presence of wide fluvial terraces north of 45°S (northern extent of the present-day course of the Río Senguerr) shows that during their formation, the major flow was coming from the north. In the region of Los Monos, the Río Senguerr abandoned the Hermoso valley during or after the deposition of the terrace T7Se (Figure 4), resulting in the present-day river flow toward the basin of the Musters and Colhué-Huapi lakes.

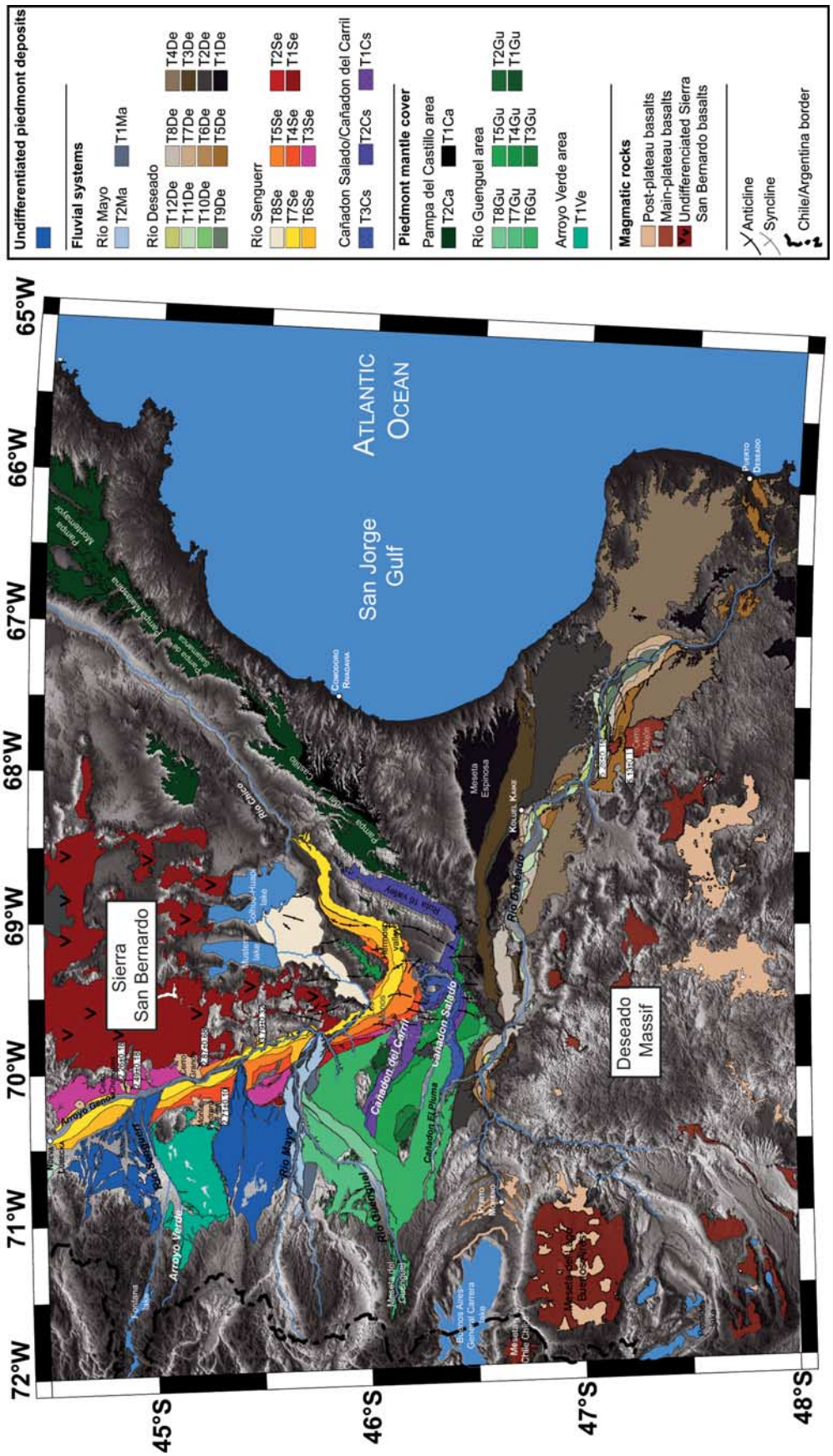

Figure 3. Map of the conglomerate surfaces covering central Patagonia. T1Ma and T2Ma, Río Mayo fluvial terraces; T1De to T12De, Río Deseado fluvial terraces; T1Se to T8Se, Río Senguerr fluvial terraces; T1Cs to T3Cs, Cañadon Saladon–Cañadon del Carril fluvial terraces; T1Ca and T2Ca, piedmont alluvial surfaces of the Pampa del Castillo area; T1Gu to T8Gu, piedmont alluvial surfaces of the Río Guenguel area; T1Ve, piedmont alluvial surface of the Arroyo Verde area.

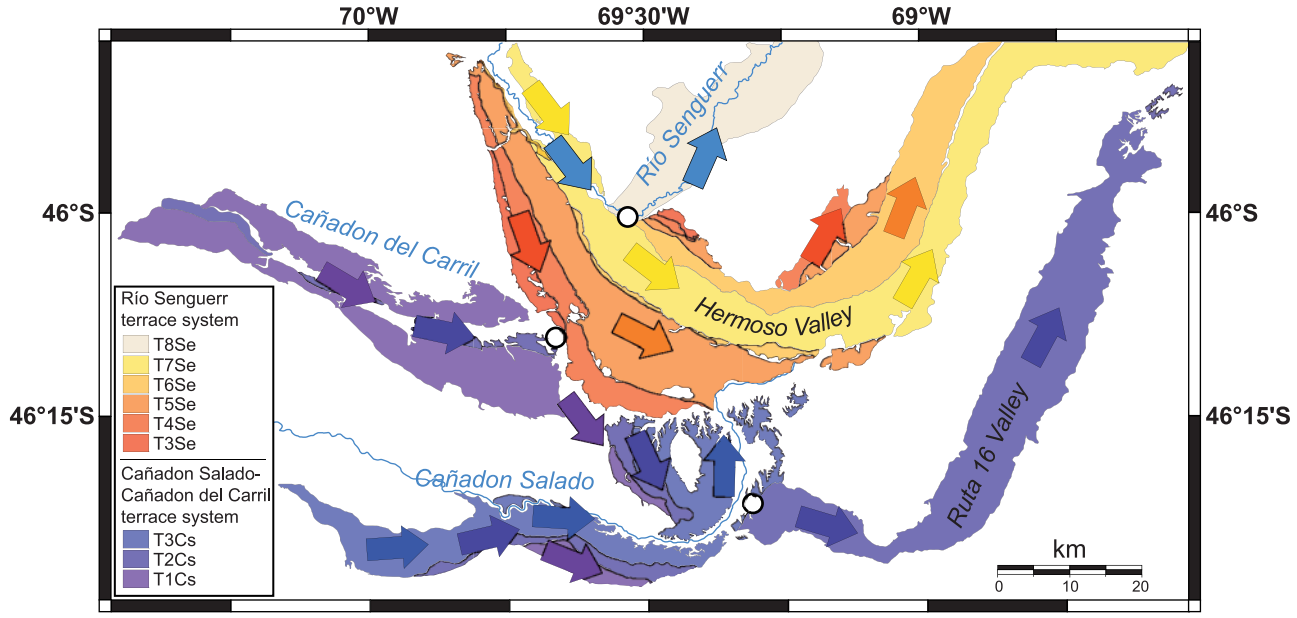

Figure 4. Stream directions during the deposition of the fluvial terraces of the Río Senguerr and Cañadon Salado–Cañadon del Carril systems. Captures are marked by white circles. Cañadon Salado and Cañadon del Carril have been captured by the paleo-Río Senguerr before the deposition of T3Cs, abandoning the Ruta 16 valley. Afterward, Río Senguerr has been captured by the Musters Lake during or just after the deposition of T7Se, abandoning the Hermoso valley.

[17] Río Deseado is a major fluvial system of the Patagonian foreland, located in the Santa Cruz province, in the southern part of the study area. Río Deseado currently originates from the region of Perito Moreno, east of the eastern edge of the Buenos Aires–General Carrera Lake, and flows on a length of 520 km to the Atlantic Ocean at Puerto Deseado. The river produced a system of twelve terraces (Figure 3). The course of the Río Deseado also changed through time, abandoning in the Meseta Espinosa, the T1De to T3De deposits tens of kilometers north of the present-day river course.

[18] In fact, all regional major river courses changed during the deposition of fluvial terrace systems. The courses of the northern rivers (Río Senguerr, Cañadon Salado) shifted northward, while the Río Deseado valley moved to the south, resulting in the present-day divergent hydrographic network. The Río Deseado now joins the Atlantic Ocean ~160 km south of the San Jorge Gulf, while the Río Senguerr flows through the Río Chico valley to the northeast and reaches the ocean ~300 km north of the San Jorge Gulf.

3.2. Age of Terraces

[19] Most of the ages proposed in the literature are relative ages based on stratigraphic relationships, which leads to discrepancy between authors. Only radiometric ages of basalt flows overlying some piedmont surfaces and fluvial terraces give some absolute constraints.

[20] All the terraces overlie the deposits of the Santa Cruz Formation and are consequently younger than ~14 Ma. Levels of piedmont mantle cover are older than the first level of each fluvial system (Río Senguerr, Cañadon Salado–Cañadon del Carril, Río Deseado). From their relative topographic position, we infer that T1Cs and T2Cs are older than T3Se, and T3Cs is at least older than T4Se and T1De.

[21] Five basalts crop out in the Río Senguerr valley. K/Ar radiometric ages have been obtained by *Bruni* [2007] in the basalts of Cerro Chenques (2.26 ± 0.11 Ma and 2.49 ± 0.18 Ma), Cerro Grande (2.87 ± 0.68 Ma) and Monte Pedrero (2.71 ± 0.10 Ma) (Figure 3). T3Se is covered by both the Cerro Chenques and Cerro Grande basalts, T4Se is covered by the Monte Pedrero basalts, and T5Se is covered by the Cerro Grande basalts. Thus, T5Se and older terraces of the Río Senguerr valley are older than 2.87 Ma and are at least middle Pliocene in age. T7Se bypasses the Cerro Grande basalts, suggesting that it formed following their emplacement and would therefore be younger than 2.87 Ma.

[22] Some absolute constraints on the age of the Río Deseado terrace system is also given by Ar/Ar radiometric ages on basalts emplaced above terraces. Ages of 5.13 ± 0.11 Ma and 5.28 ± 0.11 Ma have been obtained by *Gorring et al.* [1997] in the Cerro Monjón and Cerro Negro basalts, respectively. The Cerro Monjón basalts cover T5De, and the Cerro Negro basalts also cover younger terraces (T6De to T8De), indicating that the eight older terraces of the Río Deseado fluvial system are older than 5.28 Ma, i.e., that they are late Miocene. T9De, in contrast, is younger than 5.28 Ma and appeared during Pliocene.

[23] Figure 5 summarizes our knowledge of the age of the systems of terraces. Piedmont mantle terraces are middle to

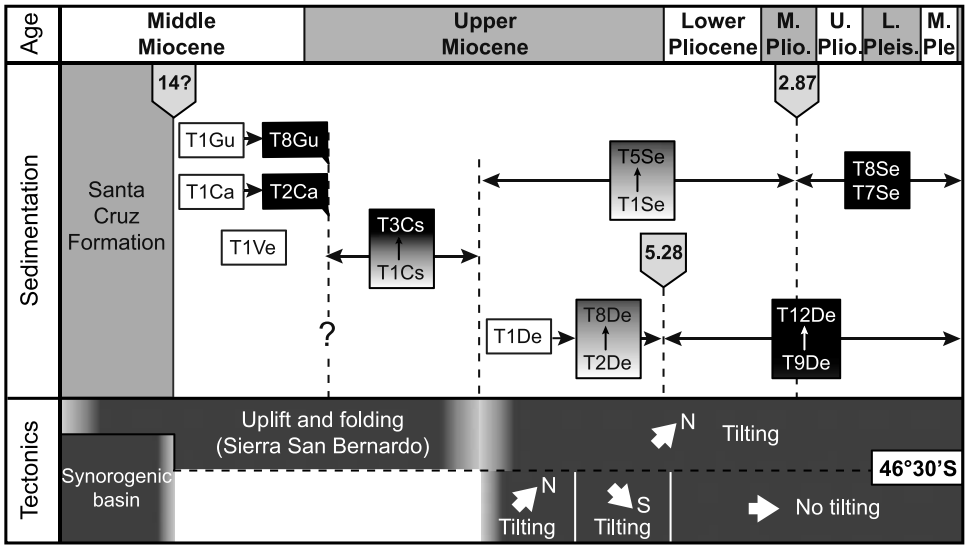

Figure 5. Age distribution of the piedmont mantle cover, fluvial terraces, and tectonic events north and south of the Chile Triple Junction. Absolute ages of basalts covering terraces are from *Gorring et al.* [1997] and *Bruni* [2007].

late Miocene in age, and the fluvial terrace system began its formation before Pliocene.

3.3. Local Tectonics

[24] As detailed above, the end of the deposition of the Santa Cruz Formation corresponds to the end of the major Oligo-Miocene shortening episode of the Cordillera. Farther east, at about 150 km from the Cordilleran thrust front, in the Sierra San Bernardo and farther south, mild deformation is attested by the presence of gentle folds and reverse faults that result from the reactivation of pre-Cretaceous extensional fault systems [*Barcat et al.*, 1989; *Homovc et al.*, 1995; *Peroni et al.*, 1995; *Chelotti*, 1997]. The San Bernardo fold belt, a 150-km-long and 50-km-wide NNW-SSE trending band, corresponds to the easternmost evidence of Andean shortening. *Rodriguez and Littke* [2001] present a detailed mapping of the folds affecting the top of the Lower Cretaceous Castillo Formation (Figure 6). Structures involve rocks of ages up to early middle Miocene, belonging to the Superpatagoniano succession, contemporaneous of the Santa Cruz Formation [*Peroni et al.*, 1995]. The San Bernardo fold belt is still today marked in the geomorphology of that part of Patagonia, locally reaching altitudes of 1500 m asl. The Río Senguerr deviates its course to the south to bypass the San Bernardo fold belt, approaching the Cañadon Salado and Río Deseado rivers.

[25] The San Bernardo folds do not deform the fluvial terraces of the Río Senguerr, showing that shortening in the Sierra San Bernardo is now inactive. However, older terrace systems are uplifted above the San Bernardo fold belt. The elevation of the piedmont cover terrace T4Gu and of the older fluvial terraces of the Cañadon Salado system (T1Cs and T2Cs) locally increases eastward approaching the western boundary of the fold belt (Figure 6). The elevation of T4Gu increases by ~90 m, and that of T1Cs of ~50 m over a distance of about 15 km. The ~E-W oriented Cañadon Salado valley is steep-sided within older piedmont terraces, evidencing that the local west directed slope of its oldest terraces does not result neither from lateral sediment supply nor from flows coming from the east (Sierra San Bernardo). Therefore, a modest-amplitude, large-wavelength uplift of the San Bernardo fold belt posterior to the formation of the Cañadon Salado–Cañadon del Carril terrace systems must have occurred, and this uplift is almost not accompanied by shortening.

3.4. Regional Tilt

[26] We studied the present-day slopes of terraces to investigate a possible long-wavelength regional uplift. If the initial downstream slope of terraces is difficult to constrain, it is reasonable to consider that terraces displayed horizontal profiles in the direction perpendicular to the paleovalleys. On the basis of this assumption, tilts would correspond to any deviation from this horizontality. Topographic profiles through terraces have been obtained using SRTM Digital Elevation Models.

3.4.1. South of the Current CTJ Position

[27] Figure 7 shows that at least the five older levels of the Río Deseado terrace system (south of 46°30′S) are inclined toward the south. The fact that steep scarps separate the different levels and that the southward slope of terrace levels is similar on both sides of the present-day Río Deseado valley shows that these slopes do not result from lateral sediment supply. In fact, southward tilt resulting from a larger regional uplift north of the terraces must have occurred to explain the observed slopes. In the N-S direction, however, T1De exhibits a slight slope toward the south ($0.05 \pm 0.01\%$) and appears locally subhorizontal. T2De and T3De, which can be followed on large distances, present a regional slope of $0.11 \pm 0.01\%$ and $0.10 \pm 0.02\%$ toward the

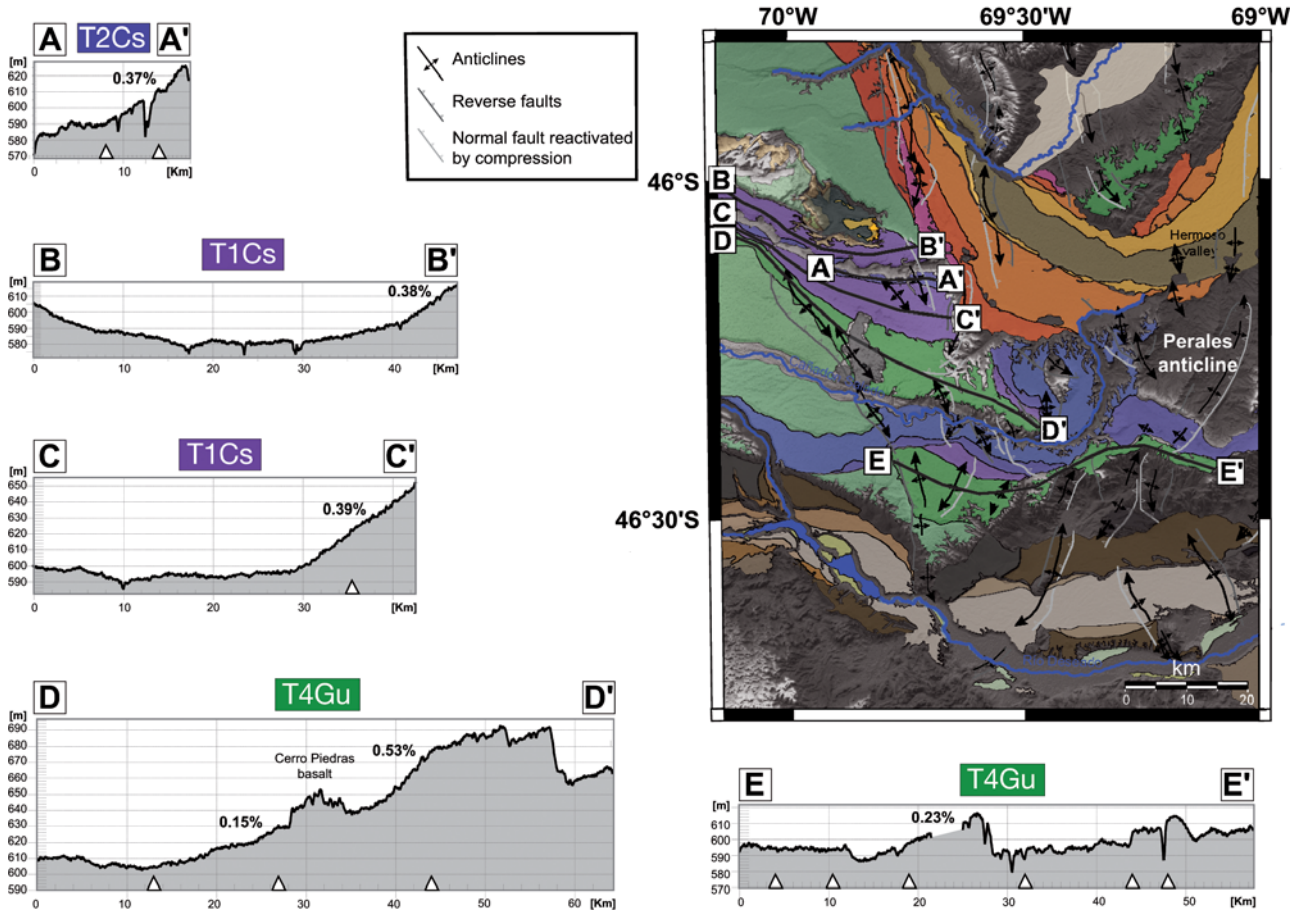

Figure 6. Topographic profiles of uplifted terraces (see map for location and Figure 3 for color legend). Vertical exaggeration is 180. T1Cs and T2Cs are for level 1 and level 2 of the Cañadon Salado–Cañadon del Carril terrace system, and T4Gu is for level 4 of the piedmont mantle cover of the Río Guenguel area. The white triangles below the topographic profiles indicate the position of the anticlines axis at the top of the Lower Cretaceous Castillo Formation [*Rodriguez and Littke*, 2001].

south, respectively, at the longitude of Koluel Kaike. The southward slope of T4De is smaller (0.07 ± 0.01% north of the Cerro Negro basalt and close to the mouth of the Río Deseado), and that of T5De, west of the Cerro Negro basalts, is even smaller (0.05 ± 0.01%). For comparison, these slopes are comparable to the longitudinal WNW-ESE trending slope of these terraces in the same area and to the present-day slope of the Río Deseado (0.08%). Terraces T6De and T7De are not extended enough to detect a potential tilt using SRTM data. The younger levels of the Río Deseado system (T8De to T12De) are not tilted. In fact, the present-day topography of the Río Deseado terrace system suggests that a gentle southward regional tilt occurred following the deposition of T3De and before T6De (or T8De). It would have been preceded by a northward regional tilt between the deposition of T1De and T2De, explaining why the present-day slope of T1De toward the south (0.05 ± 0.01%) is smaller than that of T2De (0.11 ± 0.01%). Figure 7 shows that the southward tilt that occurred between the formation of T2De and T8De resulted in the southward shift of the course of the Río Deseado, leaving abandoned the valley that resulted in the formation of T3De.

3.4.2. North of the Current CTJ Position

[28] In contrast, the analysis of the topography of terraces located just north of 46°30′S suggests that this region has essentially been tilted toward the north. East of the San Bernardo fold belt, T1Ca forms a wide planar surface that extends over 400 km from the Pampa del Castillo, west of Comodoro Rivadavia, to the Río Chico mouth to the north (Figure 8). The topography of this surface is tilted toward the northeast with a slope of 0.14 ± 0.05%. Clearly, part of the present-day slope of T1Ca results from its genesis and does not reflect subsequent tilt. However, paleocurrents observed using psephites orientations [*Beltramone and Meister*, 1992], although controversial [*Bellosi*, 1996], indicate an eastward flow direction in the Pampa del Castillo whereas the corresponding terrace is tilted toward the northeast. In addition, the present-day slope of this surface is more than three times larger than the longitudinal profile of Río Chico and larger than the longitudinal slope of other terraces that have been preserved in the eastern part of the study area (Hermoso valley, distal part of the Río Deseado terrace system). Thus, we propose that the present-day observed slope

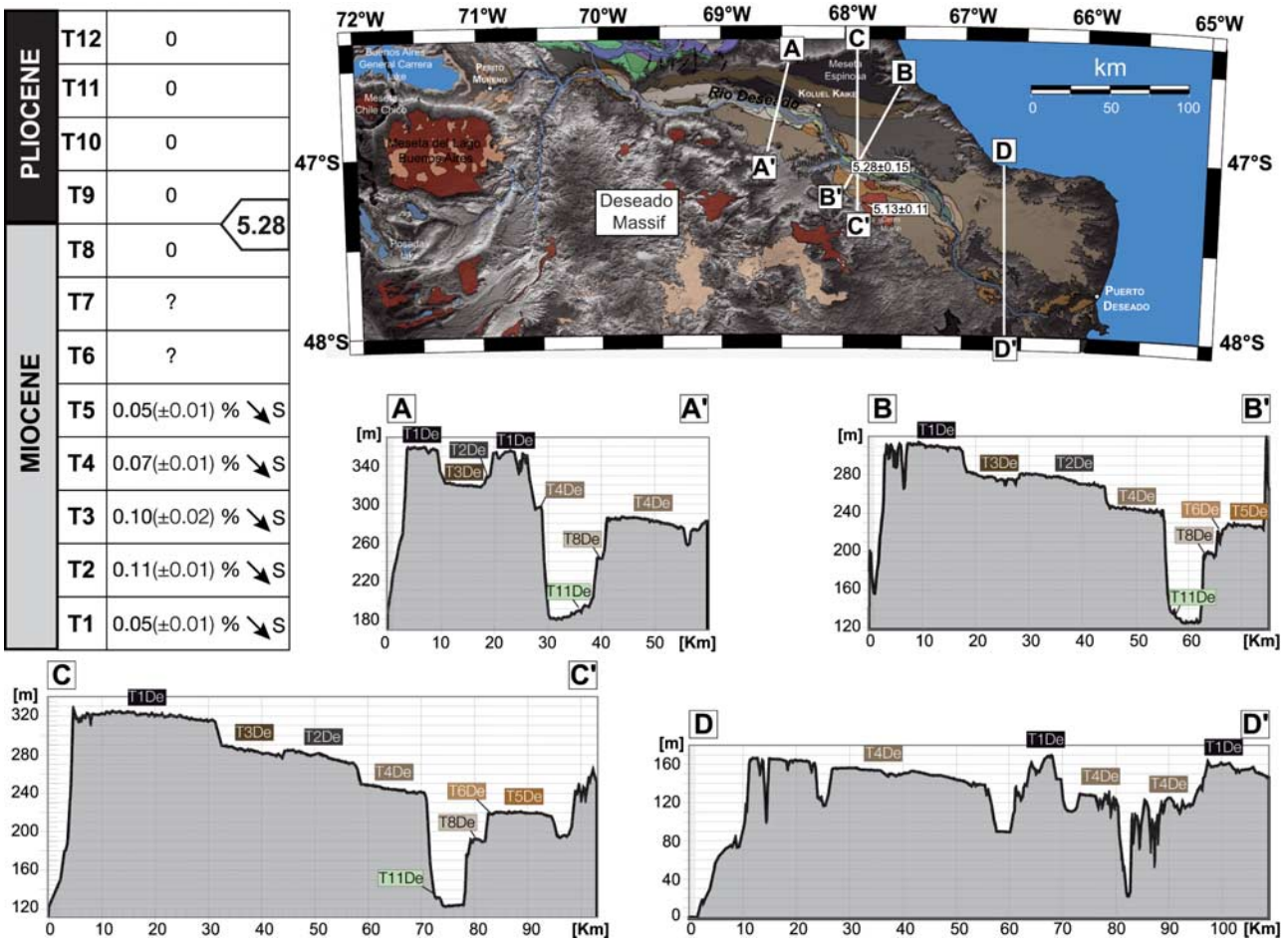

Figure 7. Topographic profiles of Río Deseado terraces (see map for location and Figure 3 for color legend) and values of N-S slope for each terrace. Numerical age of the Cerro Negro basalts is 5.28 Ma [*Gorring et al.*, 1997].

of T1Ca would partly result from a postdepositional tilt toward the north or northeast of that area.

[29] The northward tilt of the region located north of 46°30′S is also suggested by the longitudinal profile of the second terrace of the Cañadon Salado system in the Ruta 16 valley. This terrace corresponds to an abandoned valley incised within Oligo-Miocene sediments (Monte León and Santa Cruz formations). Its upstream portion is WNW-ESE oriented whereas the downstream part is directed toward the NE (Figure 8). The valley-parallel profile AA' in Figure 8 shows that the present-day longitudinal slope of that terrace is inverted toward the upstream direction in the upper WNW-ESE oriented part of the valley, whereas it goes down toward the NE in the lower part of the valley. In fact, again, this change in the slope of the terrace suggests that the area has been tilted northward. Tilting would have inverted the longitudinal slope of the part of the valley flowing toward the ESE and increased the slope of the lower part of the valley. Another possibility could be that the activity of the Sierra San Bernardo fold-and-thrust belt would have subsequently produced the uplift of the upper part of the valley and the observed counterslope for T2Cs. However, the nearest known tectonic structure along the course of T2Cs is the Perales anticline [*Homovc et al.*, 1995; *Rodriguez and Littke*, 2001] and its location at depth does not fit the change of slope observed in the Ruta 16 valley (Figure 8). Since T2Cs is not involved in any tectonic structure and since the change in its present-day slope coincides with the changing orientation of the valley, we suggest that a regional northward tilt may have caused this abnormal longitudinal profile.

[30] The longitudinal profiles of the seven terraces of the Río Senguerr system suggest that the northward tilt of the northern part of the study area pursued during their formation (Figure 9). The slope of each terrace is measured in the direction parallel to the current valley and obtained values are systematically smaller for the older terraces. For instance, T6Se lies 85 m above the present-day Río Senguerr bed just above the elbow of capture. Upstream, the difference in elevation decreases to 35 m, south of Cerro Chenques. Close to the capture, T2Se is 70 m above T6Se, while the two levels are close together 35 km NE of Cerro Chenques (Figure 9).

[31] Clearly, the higher longitudinal slope of the present-day Río Senguerr valley may also result from its capture by the Musters Lake basin. But in fact this capture may also

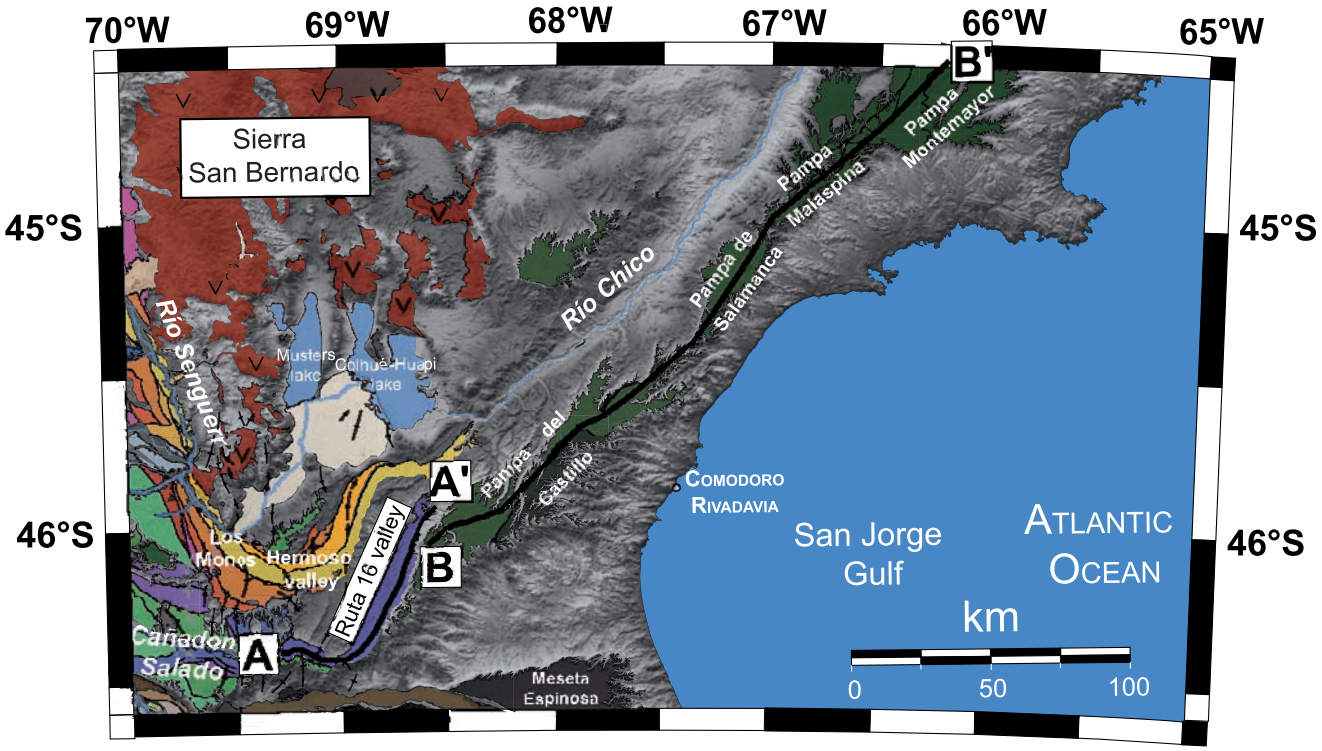
70°W
69°W
68°W
67°W
66°W
65°W
45°S
46°S
Sierra
San Bernardo
Río Chico
Pampa de Salamanca
Pampa Malaspina
Pampa Montemayor
Río Senguer
Musters lake
Colhué-Huapi lake
Pampa del Castillo
A
A'
B
B'
Ruta 16 valley
Los Monos
Hermoso valley
Cañadon Salado
Meseta Espinosa
Comodoro Rivadavia
San Jorge Gulf
Atlantic Ocean
km
0
50
100

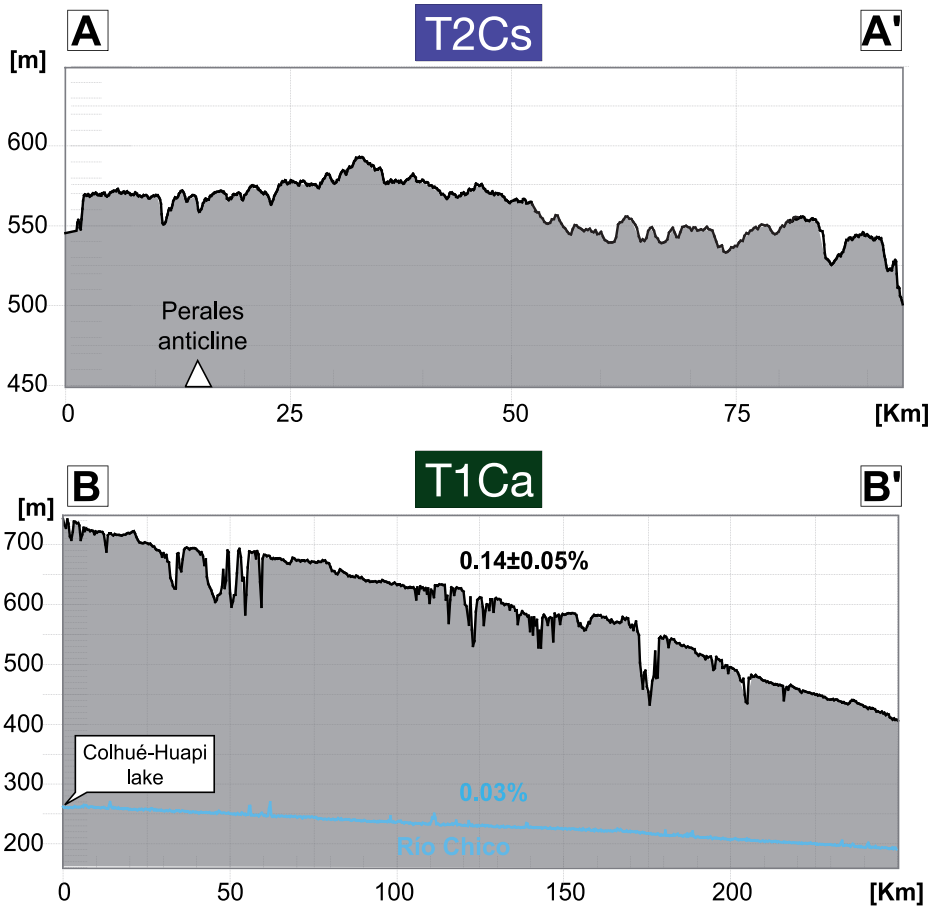
A
A'
T2Cs
[m]
600
550
500
450
Perales anticline
0
25
50
75
[Km]
B
B'
T1Ca
[m]
700
600
500
400
300
200
0.14±0.05%
Colhué-Huapi lake
0.03%
Río Chico
0
50
100
150
200
[Km]

Figure 8

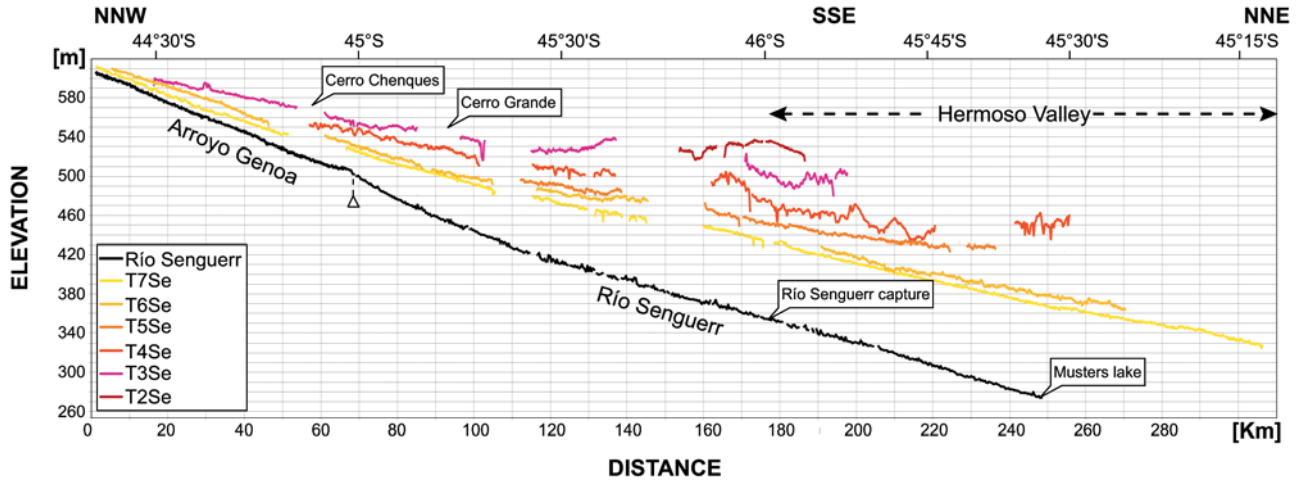

Figure 9. Topographic longitudinal profiles of the fluvial terraces of the Río Senguerr system.

have been triggered by the northward tilt of this region, as it has done for the capture of the Cañadon Salado by the Hermoso valley (Figure 4). Moreover, this capture having occurred following the formation of T7Se, it cannot explain the smaller longitudinal slopes of older terraces compared to that of T7Se. These captures would argue for a continuation of the northward tilt until recent times since the capture of the Río Senguerr postdates the deposition of the next to last terrace of the Río Senguerr fluvial system.

3.5. Synthesis of N-S Tilts Deduced From the Analysis of the Present-Day Slopes of Terraces

[32] Regions located north and south of the current CTJ position had different tilting histories from the late Miocene. In the northern area, the trench-parallel tilting is permanently northward directed and may have pursued until recent times. Absolute values of tilting are difficult to constrain since the course of the main valleys is almost parallel to the direction of tilting, the present-day slope of these terraces resulting both from tilting and from the process of terrace formation. Nevertheless, in the Río Senguerr fluvial system, if we consider that all terraces share a common upstream elevation at a latitude of 44°20′S (see Figure 9), the values of tilt can be approximated measuring the difference in elevation between the terraces at the latitude of the elbow of capture (46°S). We obtain values ranging between ~0.01 and 0.02% between successive terraces and the cumulative northward tilt between T2Se and T7Se would be ~0.06%. Present-day different slopes of the upstream and downstream segments of the older terrace T2Cs suggest a cumulative tilt of 0.12 ± 0.04% since its formation.

[33] In contrast, south of the CTJ, before 5.28 Ma, the area recorded a minimum northward tilt of 0.06 ± 0.02% (difference of N-S slope between T1De and T2De), that has been followed by a cumulative southward tilt of 0.11 ± 0.01% between T2De and T8De. Since the transition between the late Miocene and the Pliocene (T8De), southward tilting is not anymore recorded by the terraces of the Río Deseado.

[34] Both northward and southward tilts, north and south of the CTJ, resulted in captures that explain the present-day diverging pattern of the hydrographic network east of the Sierra San Bernardo and Deseado massif.

4. Possible Causes for the Post-Middle Miocene Uplift of Central Eastern Patagonia

[35] The analysis of the geological and morphological evolution of central Patagonia, east of the Andean front during the Neogene, shows a major shift from subsidence marked by the accumulation of the Santa Cruz Formation, followed by a regional uplift contemporaneous with the deposition of the piedmont mantle cover and fluvial terraces. The Oligo-Miocene transgression starts when the convergence between the Nazca and South American plates becomes more orthogonal to the margin, and is coeval to the major episode of shortening in central Patagonian Andes.

[36] Sedimentation of the Oligo-Miocene marine strata, followed by the deposition of the early to middle Miocene molasse east of the Andean front, could partly result from the flexural subsidence of the foreland induced by the growth of the chain at that time. Fission tracks data [*Thomson et al.*, 2001], indeed show that denudation accelerates in the western part of the mountain chain at that latitude in the Oligocene, which suggests that the Andes where uplifting close to the Pacific coast. We interpret the sedimentary record of the basin and especially the deposition of the Santa Cruz Formation and its equivalents, with a maximum depocenter

Figure 8. Topographic longitudinal profiles of Cañadon Salado–Cañadon del Carril terrace T2Cs (AA′) and Pampa del Castillo piedmont mantle cover level T1Ca (BB′). See map for location and Figure 3 for color legend. The present-day longitudinal slope of T2Cs depends on the orientation of the valley, suggesting that regional tilt occurred following the formation of T2Cs. The position of the Perales anticline axis is indicated by a white triangle on the profile AA′.

located close to the Cordillera foothills, as a result of the overfilling of a subsiding basin. Although the subsidence of this basin may result from the flexural response of the continental lithosphere to the growth of the Cordillera, it may also have been enhanced by the dynamic deflection of the lithosphere generated by the increasing velocity of the subduction of the Nazca slab [*Gurnis*, 1993] (see discussion below).

[37] The end of the deposition of the Santa Cruz continental series corresponds to drastic changes in the paleogeography of Patagonia. The end of early Miocene is marked by an increased aridity of the eastern side of southern Andes [*Bellosi*, 1999; *Blisniuk et al.*, 2005]. This climatic change essentially results from rain shadow phenomenon, the Cordillera being high enough to become a barrier to atmospheric circulation [*Blisniuk et al.*, 2005]. Blisniuk et al., in turn, suggest that the end of the deposition of the Santa Cruz Formation 14 Ma ago would also result from the increased aridity of the Patagonian foreland. Our data suggest that the main cause for the end of sedimentation is the uplift of the foreland. As a matter of fact, although Patagonia east of the Andes has been arid enough to preserve the fluvial terrace systems described in this paper since the late Miocene, the widespread occurrence of vast terraces covered by decimeter-scale pebbles covering the entire zone from the Andes to the Atlantic Ocean indicates that powerful streams episodically flowed from the Cordillera. These streams would certainly have brought sediments to the basin in case its subsidence would have pursued more recently than middle Miocene.

[38] Then, the question is to understand why the uplift of the Andes, controlling from the middle Miocene the semi-arid climate of eastern Patagonia, has been rapidly followed by the slow uplift of its foreland. Uplift of central eastern Patagonia correlates with a period of colder climate, culminating with the formation of an ice cap above the Andes. The long-term increasing ice load from the upper Miocene should have triggered subsidence of the Andean foreland, contrary to the observed uplift. In contrast, foreland uplift may have resulted from a decreasing load of the Cordillera, possibly enhanced by glacial erosion. We show below that flexural foreland rebound cannot explain the large dimension of the uplifted area. In contrast, dynamic topography resulting from the opening of the asthenospheric window may explain the continental-scale observed uplift.

4.1. Flexural Response of the Lithospheric Plate

[39] The growth of southern Andes in the Oligo-Miocene resulted from crustal shortening, which, in turn, triggered subsidence in the foreland and deposition of the Santa Cruz molasse [e.g., *Ramos*, 1989; *Alvarez-Marrón et al.*, 1993; *Thomson et al.*, 2001; *Kraemer et al.*, 2002; *Lagabrielle et al.*, 2004; *Ramos*, 2005]. Then, the subsequent uplift of the foreland may have resulted from the diminution of the Andean load above the continental plate. As a matter of fact, crustal shortening has been very small in the Patagonian Andes since middle Miocene [*Ramos*, 1989; *Coutand et al.*, 1999; *Lagabrielle et al.*, 2004, 2007]. Moreover, the very humid climatic conditions on the western side of the chain that has been enhanced by its uplift, and the development of Neogene glaciations may have increased the rapid erosion of the Pacific side of the continent and central part of the Cordillera. The flexural response of these accelerated erosion processes would favor uplift of the eastern foreland.

[40] The elastic thickness of the Patagonian continental lithosphere has been estimated between about 20 km and 30 km by *Tassara et al.* [2007] at the CTJ latitude using gravity data. Using standard elastic parameters [e.g., *Turcotte and Schubert*, 1982], the distance between the chain and the forebulge would range between 150 and 210 km. Flexural parameters of the continental plate are also evidenced by the distribution of the Santa Cruz continental deposits, which are restricted to the western part of the Patagonian foreland, less than 250 km from the Andes. In turn, the flexural uplift of the foreland resulting from the diminution of the Andean load should be restricted to a narrow area close to the chain, and should not affect the distal zones close to the Atlantic coast, ~500 km away from the present-day Cordillera.

4.2. Dynamic Topography

[41] Dynamic topography on Earth is the deflection of the surface in response to the viscous flow that occurs in the convecting underlying mantle. Over subduction zones, it may result in long-wavelength downward deflections of the overriding topographic surface exceeding 1000 m [*Mitrovica et al.*, 1989; *Gurnis*, 1993; *Zhong and Gurnis*, 1994; *Husson*, 2006]. The northward migration of the CTJ from middle Miocene lead to the opening of an asthenospheric window below southern Patagonia. South of 46°30′S, the Antarctic oceanic plate is now slowly subducting below the continent. The corresponding slab is short. A recent slab window reconstruction shows that the Antarctic slab should not have reached depths greater than 45 km [*Breitsprecher and Thorkelson*, 2008]. Thus, the dynamic effect of that subduction on the overriding continent is virtually absent. North of the CTJ, in contrast, the Nazca plate subducts rapidly, which in turn deflects the continental plate downward. We propose that this downward deflection has been progressively canceled in southern Patagonia as the CTJ was migrating northward, resulting in the uplift of that part of the continent. The free air anomaly is positive north of the CTJ (40 mGal) while it is neutral to slightly negative south of it; this observation outlines the departure of topography from an isostatic situation north of the CTJ and the fact that the dynamic deflection vanishes south of it.

[42] We computed the dynamic deflection induced by a slab subducting within the upper mantle with a dip angle of 37°, using a simple 3-D Newtonian model based on the Stokeslet approximation [*Morgan*, 1965; *Batchelor*, 1967; *Harper*, 1984; *Husson*, 2006]. A subducting slab of finite width is discretized into elementary spheres, or "Stokeslet," for which an analytical flow solution exists. Each point mass i induces an elementary spherical flow (Stokeslet) for which the Stokes stream function is known and can be written $\Psi_i = (\Delta\rho v_i g/8\pi\eta) r_{ij} \sin^2 \theta_{ij}$, where $\Delta\rho v_i$ is the mass anomaly associated with each point mass, g is the gravitational acceleration, η is the viscosity, r_{ij} is the distance from each point mass to the observation point j, and θ_{ij} is the angle between the vector ij and the direction of g. The normal

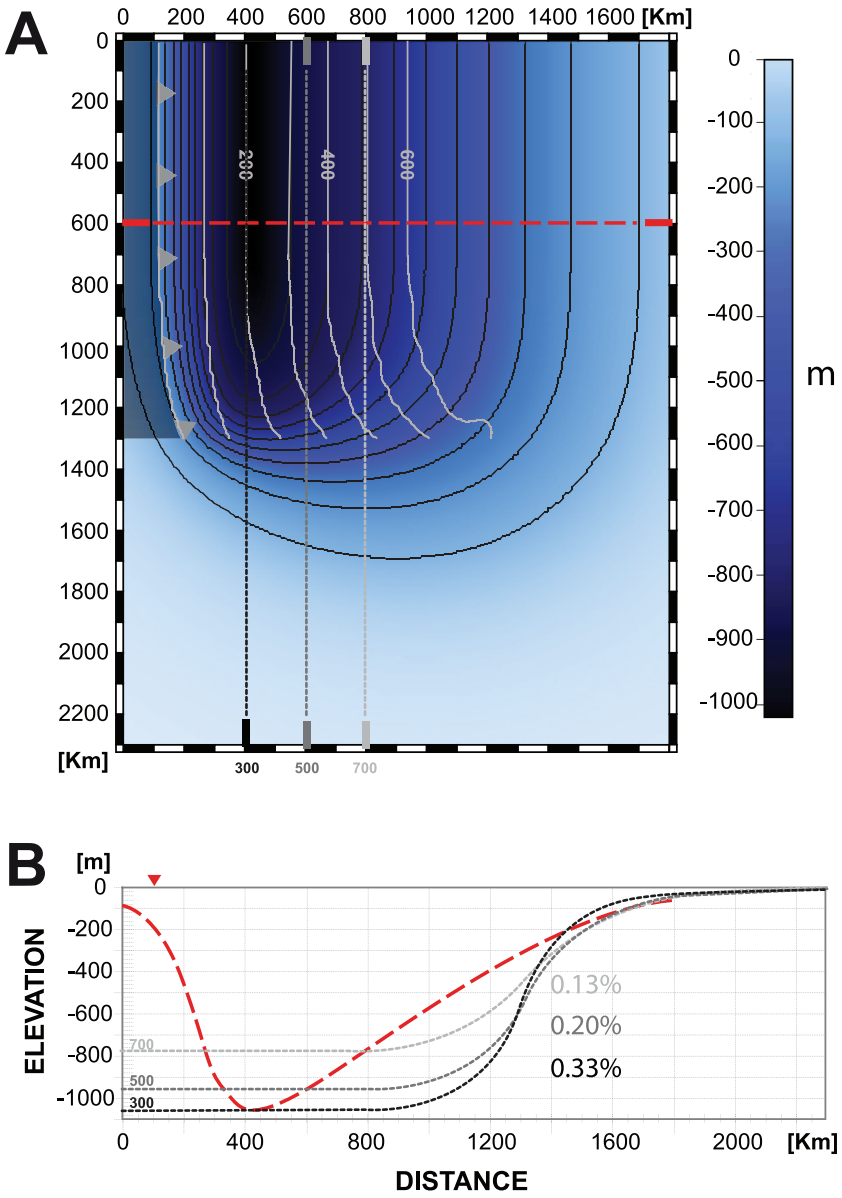

Figure 10. (a) Topographic deflections induced by the subduction of a semi-infinite, 50-km-thick negatively buoyant slab ($\Delta\rho = -80$ kg m^{-3}, steady state slab dip of 37°). Black solid lines are isodepth contours of topographic deflection and gray solid lines show the depth of the subducting slab (in km). The gray solid line with triangles indicates the position of the trench. (b) Topographic profiles of the dynamic topography, in the direction parallel to the trench, at a distance of 300 km (black dotted line), 500 km (dark gray dotted line), and 700 km (light gray dotted line) from the trench, and in the direction perpendicular to the trench (dashed line), with the corresponding trench-parallel slopes indicated on the right. Profiles are positioned on Figure 10a, and the location of the trench is indicated by a triangle.

stress on the upper free surface of a half-space can be calculated using the image technique [*Morgan*, 1965]. It writes $Fzz_{ij} = 3\Delta\rho v_i g z_i^3/\pi r_{ij}^5$, where z_i is the depth of the point mass body beneath the surface. Because inertial terms are negligible, stress does not depend on viscosity. If the surface is stress free, then there will instead be a deflection of the surface by a distance h_{ij}, such that $h_{ij} = Fzz_{ij}/\rho_m g$. The total Stokes flow is given by the sum of the Stokeslets; in aerial domains the total surface deflection H_j will be the sum of the deflections resulting from each point mass; hence,

$$H_j = \sum_i \frac{3\Delta\rho v_i z_i^3}{\pi r_{ij}^5 \rho_m}, \quad (1)$$

where ρ_m denotes the density of the mantle.

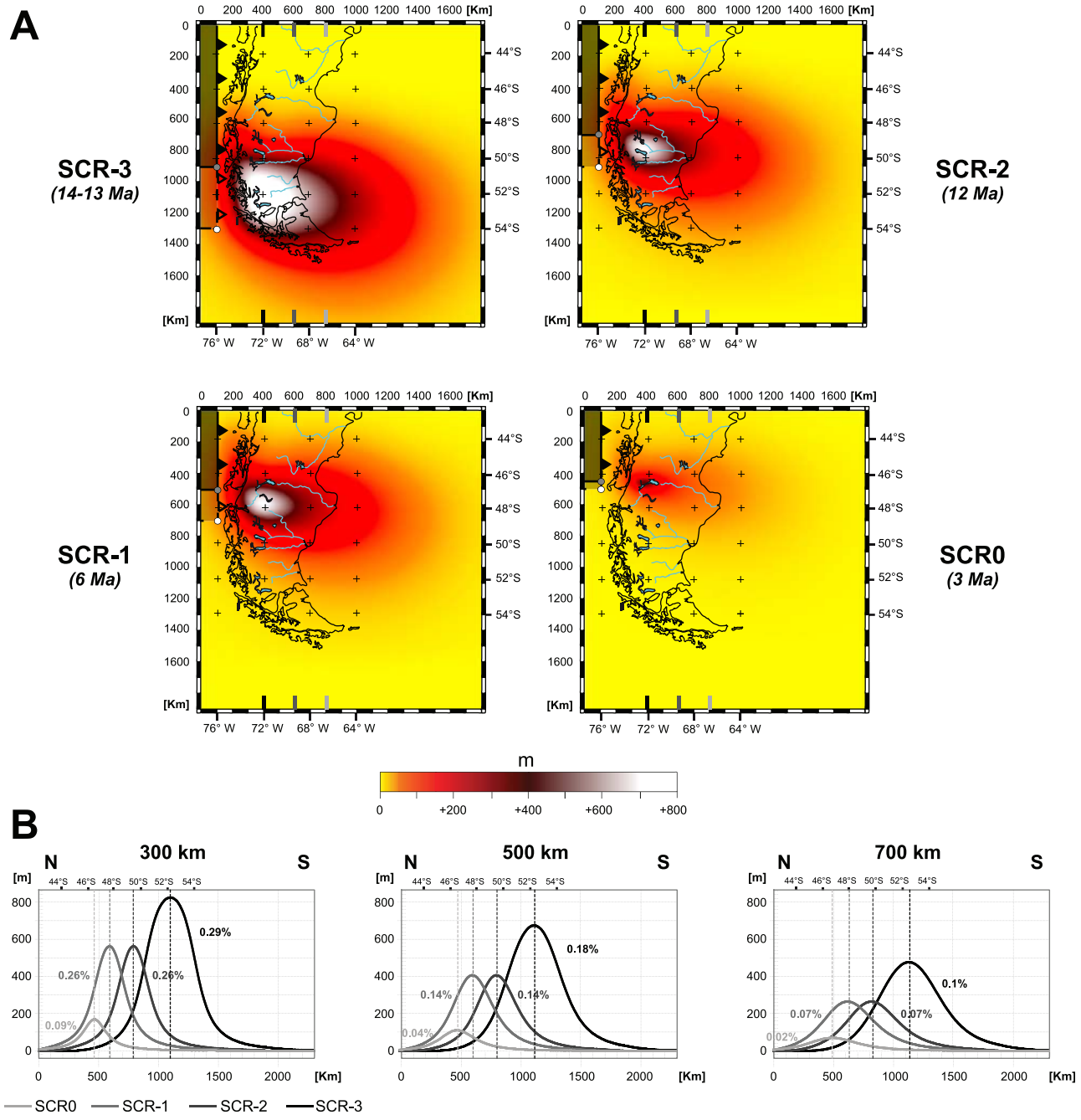

Figure 11. (a) Map of the uplift of the overriding plate resulting from the episodic subduction of 4 ridge segments below South America accompanying the northward migration of the CTJ. White and gray dots mark the position of the CTJ before and after the subduction of each ridge segment, respectively. (b) Topographic profiles parallel to the trench direction at 300 km, 500 km, and 700 km from the trench for each triple junction migration increment. The boundary between regions of northward and southward tilt for each longitudinal profile (dotted lines) shifts toward the north, delineating sectors with different tilt history.

[43] Deflections have been calculated for a 50-km-thick slab with a negative buoyancy of -80 kg m^{-3}. We assume that the deflection, south of the triple junction, is null. This is supported by the fact that the Antarctic slab currently reaches depths smaller than 45 km [*Breitsprecher and Thorkelson*, 2008]. Conversely, the dynamic effect of the trailing edge of the Nazca slab south of the CTJ should not be negligible but is difficult to quantify since it depends on many poorly constrained parameters like the slab geometry, the convergence velocity, the rheological stratification of the

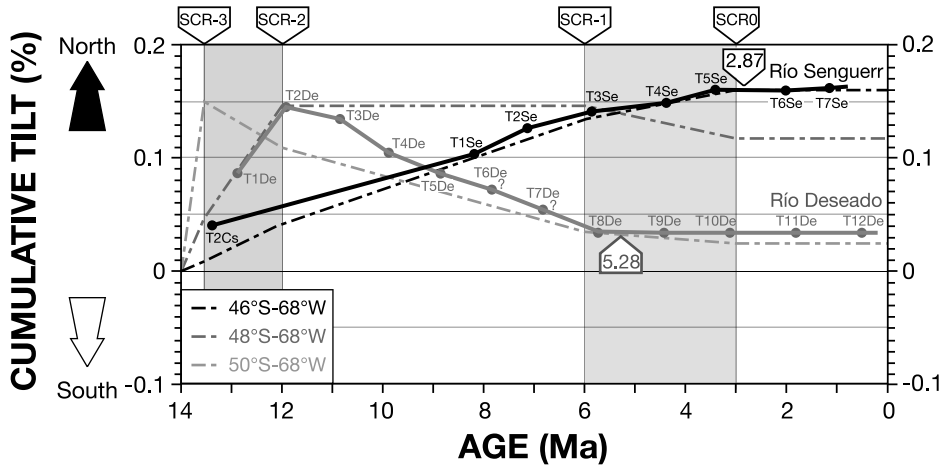

Figure 12. Modeled versus observed tilts in the central eastern Patagonia during the last 14 Ma. Dash-dotted lines indicate the predicted cumulative tilt at 46°S–68°W (black), 48°S–68°W (dark gray), and 50°S–68°W (light gray). The corresponding observed cumulative tilts observed in terraces south (Río Deseado), and north of the CTJ (Río Senguerr and Cañadon Salado) are indicated by light gray and black solid lines, respectively. Note that the ages of terraces are not known. We only know their stratigraphic position with respect to 5.28 Ma old basalts in the Río Deseado fluvial system [*Gorring et al.*, 1997], and 2.87 Ma old basalts in the Río Senguerr fluvial system [*Bruni*, 2007].

upper mantle, thermal erosion of the slab edge. Anyway, its effect would only introduce a delay between ridge subduction at trench, and dynamic uplift. A first-order approximation of this delay can be evaluated calculating the time necessary for the horizontal projection of the trailing edge of the slab to reach an horizontal distance greater than that of the central Patagonian basin (∼5 Ma).

[44] Analytical calculations predict that vertical deflections appear as far as 1600 km from the trench and reach a maximum value close to 1000 m at a distance of ∼325 km from the trench. The maximum N-S trending surface slope at a distance of 300, 500, and 700 km from the trench is ∼0.33%, 0.2%, and 0.13%, respectively (Figure 10). The amplitude of the deflection varies when parameters (thickness, buoyancy, and dip of the slab) are changed but the general observed pattern is maintained.

[45] The CTJ abruptly migrates northward when ridge segments enter the subduction zone. From middle Miocene, several ridge segments subducted below the southern Andes (Figure 1). We model the dynamic response of the subduction of four ridge segments with lengths of 400, 200, 200, and 50 km that correspond to the lengths of SCR-3, SCR-2, SCR-1, and SCR0 (South Chile Ridge segments), respectively. These segments subducted beneath South America 13.5, 12, 6, and 3 Ma ago, respectively [*Cande and Leslie*, 1986; *Gorring et al.*, 1997]. Figure 11a is a map view of surface uplift resulting from the subduction of each ridge segment, subsequent quasi cessation of the subduction and induced dynamic deflection. Figure 11b presents the corresponding uplift along three trench-parallel profiles located 300, 500, and 700 km from the trench. Uplift is maximum in front of each subducted ridge segment, resulting in northward tilt north of the segment and southward tilt south of it. Southern Patagonia can be divided into four domains. The first domain, located to the north, experienced a constant northward tilt during the whole migration of the triple junction. The three other domains first tilted northward and then southward as the CTJ was migrating to the north.

4.3. Discussion

[46] The calculations presented above show that dynamic topography resulting from subduction may result in significant long-wavelength deflections of the lithospheric plate, far enough from the trench to affect the entire width of Patagonia. At the end of Oligocene, the increase of trench-perpendicular convergence velocity between the Farallon-Nazca plate and South America may have resulted in a larger downward deflection of the continental plate, which would explain part of the Oligo-Miocene Patagonian transgression.

[47] Following the deposition of the Miocene continental molasse, the entire continental plate uplifted, resulting in the appearance of continental-scale terraces. Available ages on basalts covering terraces [*Gorring et al.*, 1997; *Bruni*, 2007] show that the older terraces are middle-late Miocene, and that only the lower terraces of the Río Senguerr and Río Deseado fluvial systems are Pliocene to Pleistocene. The present-day topography of these ancient terraces underlines periods of northward and southward tilt in the foreland of the Patagonian Andes. South of 46°30′S, terraces of the Río Deseado system evidence a former 0.06% northward tilt event (0.11% minus 0.05%) that occurred before the deposition of T2De, and partly following the deposition of T1De, followed by a 0.11% southward tilt that followed the deposition of T2De and ended before the deposition of T8De, i.e., before 5.28 Ma. Just to the north of 46°30′S (Cañadon Salado and Río Senguerr terrace systems), the oldest surfaces are tilted toward the north, and the northward tilt recorded by the youngest terraces of the Río Senguerr fluvial

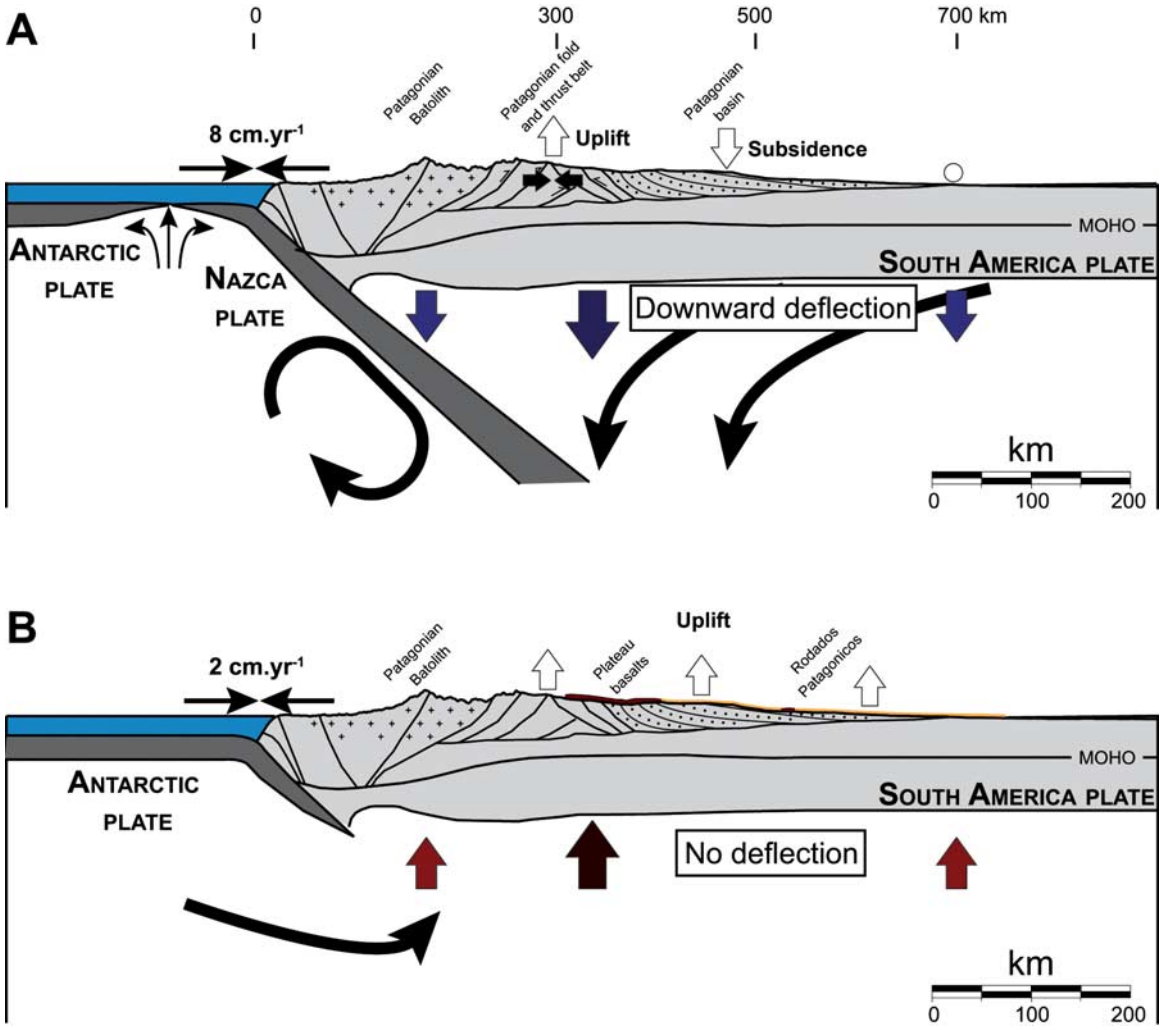

Figure 13. Cartoons illustrating the geodynamic setting south of the Chile Triple Junction. (a) Before the subduction of the Chile ridge, the Nazca slab subduction induces mantle flow that causes a downward deflection of the overlying Patagonian lithosphere. The rapid convergence rate is responsible for the emplacement of the eastern Patagonian fold and thrust belt and associated subsiding flexural basin. (b) After the subduction of the Chile ridge, the opening of the asthenospheric window cancels the downward mantle motion that deflected the South American plate, resulting in the uplift of the continent at that time.

system indicates that the tilt continued after the deposition of the Cerro Grande basalts, 2.87 Ma ago.

[48] This general pattern of tilt basically reproduces the predicted vertical movements from dynamic topography modeling (Figure 12) that accommodate the northward migration of the CTJ: south of the CTJ, our model predicts that the uplift is accommodated by northward tilt followed by southward tilt, and north of the CTJ, only northward tilt should occur. Moreover, observed tilt values are approximately 0.1% at the longitude of the Atlantic coast, which corresponds to the range of values predicted by the semianalytical models.

[49] However, model results suggest that southward tilt of the region located between 46°30′S and 48°S would occur following the final step of migration of the CTJ that resulted from the subduction of the SCR0 ridge segment, 3 Ma ago. Moreover, as discussed above, our simple analytical model does not integrate the effect of the trailing edge of the Nazca slab at depth, south of the triple junction, which should introduce a delay between ridge subduction and the corresponding dynamic response. Ages of the Río Deseado fluvial system, in contrast, suggest that the southward tilt occurred in the Miocene, before the deposition of the 5.28 Ma old Cerro Negro basalts. This discrepancy outlines the limitation of our simple analytical analysis in explaining the timing and/or location of observed tilt. In the semianalytical model presented above, dynamic deflections are computed for a slab having an uniform buoyancy while the Nazca slab is in fact younger and therefore less negatively buoyant next to the CTJ. Thus, taking precisely into account the age structure of the subducting slab would subsequently shift the maximum deflection northward with respect to

model results (Figure 11) and southward tilt would occur earlier.

[50] Another possibility is that the migration of the CTJ has been preceded by a slab break-off, resulting in the opening of an asthenospheric window before the subduction of the last ridge segments, as already proposed by *Guivel et al.* [2006] to explain the occurrence of back-arc basalts older than the subduction of the ridge segments located at their latitude. Although the model could easily be adapted accordingly, such improvements would remain beyond the resolution of the model itself.

[51] *Ramos* [1989, 2005], *Ramos and Kay* [1992], and *Lagabrielle et al.* [2007] point out a striking difference in the elevation of the highest peaks of the Cordillera, they relate with the opening of the slab window beneath the continent. North of the CTJ, highest Cordillera peaks do not exceed 2500 m, whereas south of the CTJ, numerous peaks exceed 3000 m. Although larger amounts of uplift (>1000m) are indeed expected close to the Andes according to the analytical model, the signal is more difficult to decipher because of the tectonic activity, large erosion rates and the isostatic rebound related to episodic melting of late Miocene to Quaternary glaciers that make any attempt to extract a reference level dubious.

5. Conclusions

[52] The major Oligo-Miocene transgression that occurred in the southern Patagonia results both from shortening of the Cordillera and larger downward dynamic deflection of the continental plate resulting from the increase of the trench-perpendicular convergence velocity between the subducting and overriding plates (Figure 13). The Santa Cruz Formation deposited in the overfilled subsiding Patagonian basin. The middle Miocene time is characterized by a switch from subsidence to uplift of the Andean foreland. Terraces overlaid by coarse fluvial series are found across the entire continent, from the Andes to the Atlantic Ocean. They mark a generalized uplift of the continental plate that started in the middle-late Miocene when the overall subduction dynamics changed. Although part of this uplift, close from the Andes, could possibly result to some extent from the flexural response of the continental lithosphere to the erosion of the chain and subsequent unloading, dynamic topography resulting from mantle–lithosphere interaction is necessary to explain uplift occurring on larger wavelengths, from the Andes to the Atlantic coast. The episodic northward migration of the Chile Ridge Triple Junction, resulting in the opening of a slab window below southern Patagonia, cancels the dynamic downward deflection of the continental plate above the subduction zone and induces the uplift (or better said the cessation of the dynamic defection) of the overriding plate (Figure 13). The uplift resulting from the dynamic response of the continental lithosphere to subduction explains the diverging present-day pattern of the hydrographic network at the latitude of the CTJ, the region located north of the CTJ being tilted northward while the region located to the south tilts toward the south. The comparison between the model and the observations show that both the occurrence of the Patagonian basin and its evolution are of dynamic origin.

[53] **Acknowledgments.** This research was supported by the French CNRS-INSU "Reliefs de la Terre" program. The authors thank Serge Lallemand and two anonymous reviewers for a complete and detailed review of a previous version of this paper. They thank IRD (Institut de la Recherche pour le Développement) for help in organizing the field work and Silvia Espinach (Universidad de Buenos Aires) for field assistance. This work benefited from fruitful discussions with R. Giacosa (Universidad de Comodoro Rivadavia) and Ernesto Cristallini (Universidad de Buenos Aires).

References

Airy, G. B. (1855), On the computation of the effect of the attraction of mountain-masses as disturbing the apparent astronomical latitude of stations in geodetic surveys, *Philos. Trans. R. Soc. London*, *145*, 101–104, doi:10.1098/rstl.1855.0003.

Alvarez-Marrón, J., K. R. McClay, S. Harambour, L. Rojas, and J. Skarmeta (1993), Geometry and evolution of the frontal part of the Magallanes foreland thrust and fold belt (Vicuña area), Tierra del Fuego, southern Chile, *AAPG Bull.*, *77*, 1904–1921.

Ardolino, A., J. L. Panza, and E. Yllañez (2003), Hoja Geológica 4566-I Garayalde, provincia del Chubut, scale , 1:250000, Serv. Geol. Minero Argent., Buenos Aires.

Batchelor, G. (1967), *An Introduction to Fluid Mechanisms*, 615 pp., Cambridge Univ. Press, Cambridge, U. K.

Barcat, C., J. S. Cortiñas, V. A. Nevistic, and H. E. Zucchi (1989), Cuenca del Golfo San Jorge, in *Cuencas Sedimentarias Argentinas*, *Ser. Correl. Geol.*, vol. 6, edited by G. Chebli and L. Spaletti, pp. 319–345, Univ. Nac. de Tucumán, Tucumán, Argentina.

Barreda, D. V., and I. Caccavari (1992), Mimosoideae (Leguminosae) occurrences in the early Miocene of Patagonia (Argentina), *Palaeogeogr. Palaeoclimatol. Palaeoecol.*, *94*, 243–252, doi:10.1016/0031-0182(92)90121-K.

Bellosi, E. S. (1996), Fabrica de los "rodados patagónicos" y paleocorrientes: Comentario y replica, *Asoc. Geol. Argent. Rev.*, *51*(1), 87–89.

Bellosi, E. S. (1999), El Cambio climático-ambiental de la Patagonia en el Mioceno temprano-Medio, paper presented at 14th Congreso Geológico Argentino, Asoc. Geol. Argent., Salta, Argentina.

Bellosi, E. S., and D. V. Barreda (1993), Secuencias y Palinología del Terciario medio en la cuenca San Jorge, registro de oscilaciones eustáticas en Patagonia, paper presented at 12th Congreso Geológico Argentino and 2nd Congreso Exploración de Hidrocarburos, Asoc. Geol. Argent., Mendoza, Argentina.

Beltramone, C., and C. M. Meister (1992), Paleocorrientes de los Rodados Patagónicos, tramo Comodoro Rivadavia—Trelew, *Asoc. Geol. Argent. Rev.*, *47*(2), 147–152.

Bianchi, J. L. (1981), Cuenca del Golfo San Jorge. Su genesis e interconexiones, *Petrotecnia*, *Agosto 1981*, 27–35.

Blisniuk, P. M., L. B. Stern, C. P. Chamberlain, B. Idleman, and P. K. Zeitler (2005), Climatic and ecologic changes during Miocene surface uplift in the southern Patagonian Andes, *Earth Planet. Sci. Lett.*, *230*, 125–142, doi:10.1016/j.epsl.2004.11.015.

Breitsprecher, K., and D. J. Thorkelson (2008), Neogene kinematic history of Nazca-Antarctic-Phoenix slab windows beneath Patagonia and the Antarctic Peninsula, *Tectonophysics*, *464*, 10–20, doi:10.1016/j.tecto.2008.02.013.

Bruni, S. (2007), The Cenozoic back-arc magmatism of central Patagonia (44°–46°S): Activation of different mantle domains in space and time, Ph.D. thesis, 159 pp., Univ. di Pisa, Pisa, Italy.

Čadek, O., and L. Fleitout (2003), Effect of lateral viscosity variations in the top 300 km on the geoid and dynamic topography, *Geophys. J. Int.*, *152*, 566–580, doi:10.1046/j.1365-246X.2003.01859.x.

Cande, S., and R. B. Leslie (1986), Late Cenozoic tectonics of the southern Chile Trench, *J. Geophys. Res.*, *91*, 471–496, doi:10.1029/JB091iB01p00471.

Catuneanu, O., C. Beaumont, and P. Waschbusch (1997), Interplay of static loads and subduction dynamics in foreland basins: Reciprocal stratigraphies and the "missing" peripheral bulge, *Geology*, *25*(12), 1087–1090, doi:10.1130/0091-7613(1997)025<1087:IOSLAS>2.3.CO;2.

Cembrano, J., A. Lavenu, P. Reynolds, G. Arancibia, G. López, and A. Sanhueza (2002), Late Cenozoic transpressional ductile deformation north of the Nazca-South America-Antarctica triple junction, *Tectonophysics*, *354*, 289–314, doi:10.1016/S0040-1951(02)00388-8.

Chelotti, L. (1997), Evolución tectónica de la Cuenca del Golfo San Jorge en el Cretácico y Terciario: Algunas observaciones desde la interpretación sísmica, *Bol. Inf. Petrol.*, *49*, 62–82.

Cobos, J. C., and J. L. Panza (2001), Hoja Geológica 4769-III El Pluma, provincia de Santa Cruz, scale, 1:250000, Serv. Geol. Minero Argent., Buenos Aires.

Coutand, I., M. Diraison, P. R. Cobbold, D. Gapais, E. A. Rossello, and M. Miller (1999), Structure

and kinematics of a foothills transect, Lago Viedma, southern Andes (49°30S), *J. South Am. Earth Sci.*, *12*, 1–15, doi:10.1016/S0895-9811(99)00002-4.

Dal Molin, C., M. Márquez, and B. Maisonabe (1998), Hoja Geológica 4571-IV Alto Río Senguerr, provincia del Chubut, scale, 1:250000, Serv. Geol. Minero Argent., Buenos Aires.

De la Cruz, R., and M. Suárez (2006), Geología del área Puerto Guadal-Puerto Sánchez, Región Aisén del General Carlos Ibañez del Campo, in *Carta Geológica de Chile*, *Ser. Geol. Básica*, vol. 95, 58 pp., scale, 1:100000, Serv. Nac. de Geol. y Minería, Santiago, Chile.

De Mets, C., R. C. Gordon, D. F. Argus, and S. Stein (1994), Effect of recent revisions to the geomagnetic reversal time scale on estimates of current plate motions, *Geophys. Res. Lett.*, *21*, 2191–2194, doi:10.1029/94GL02118.

D'Orazio, M., S. Agostini, F. Mazzarini, F. Innocenti, P. Manetti, M. J. Haller, and A. Lahsen (2000), The Pali Aike Volcanic Field, Patagonia: Slab-window magmatism near the tip of South America, *Tectonophysics*, *321*, 407–427, doi:10.1016/S0040-1951(00)00082-2.

D'Orazio, M., S. Agostini, F. Innocenti, M. J. Haller, P. Manetti, and F. Mazzarini (2001), Slab window-related magmatism from southernmost South America: The late Miocene mafic volcanics from the Estancia Glencross area (~52°S, Argentina-Chile), *Lithos*, *57*, 67–89, doi:10.1016/S0024-4937(01)00040-8.

D'Orazio, M., F. Innocenti, P. Manetti, M. Tamponi, S. Tonarini, O. González-Ferrán, A. Lahsen, and R. Omarini (2003), The Quaternary calc-alkaline volcanism of the Patagonian Andes close to the triple junction: Geochemistry and petrogenesis of volcanic rocks from the Cay and Maca volcanoes (~45°S, Chile), *J. South Am. Earth Sci.*, *16*, 219–242, doi:10.1016/S0895-9811(03)00063-4.

D'Orazio, M., F. Innocenti, P. Manetti, M. J. Haller, G. Di Vicenzo, and S. Tonarini (2005), The late Pliocene mafic lavas from the Camusú Aike Volcanic Field (~50°S, Argentina): Evidences for geochemical variability in slab window magmatism, *J. South Am. Earth Sci.*, *18*, 107–124, doi:10.1016/j.jsames.2004.10.001.

Escosteguy, L., C. Dal Molin, M. Franchi, S. Geuna, and O. Lapido (2003), Hoja Geológica 4772-II Lago Buenos Aires, provincia de Santa Cruz, scale , 1:250000, Serv. Geol. Minero Argent., Buenos Aires.

Espinoza, F., et al. (2005), Petrogenesis of the Eocene and Mio-Pliocene alkaline basaltic magmatism in Meseta Chile Chico, southern Patagonia, Chile: Evidence for the participation of two slab windows, *Lithos*, *82*, 315–343, doi:10.1016/j.lithos.2004.09.024.

Feruglio, E. (1950), *Descripción Geológica de la Patagonia*, vol. III, Yacimientos Petrol. Fis., Buenos Aires, Argentina.

Flint, S. S., D. J. Prior, S. M. Agar, and P. Turner (1994), Stratigraphic and structural evolution of the Tertiary Cosmelli Basin and its relationship to the Chile Triple Junction, *J. Geol. Soc.*, *151*, 251–268, doi:10.1144/gsjgs.151.2.0251.

Flynn, J. J., M. J. Novacek, H. E. Dodson, D. Frassinetti, M. C. McKenna, M. A. Norell, K. E. Sears, C. C. Swisher, III, and A. R. Wyss (2002), A new fossil mammal assemblage from the southern Chilean Andes: Implications for geology, geochronology, and tectonics, *J. South Am. Earth Sci.*, *15*, 285–302, doi:10.1016/S0895-9811(02)00043-3.

Frassinetti, D., and V. Covacevich (1999), Fauna de invertebrados fósiles marinos de la Formación Guadal en Pampa Castillo, sur del Lago General Carrera, Aisén, Chile, *Bol. Serv. Nac. Geol. Minería*, *51*, 1–96.

Froidevaux, C., and B. L. Isacks (1984), The mechanical state of the lithosphere in the Altiplano-Puna segment of the Andes, *Earth Planet. Sci. Lett.*, *71*, 305–314, doi:10.1016/0012-821X(84)90095-5.

Garzione, C. M., P. Molnar, J. C. Libarkin, and B. J. Mac Fadden (2006), Rapid late Miocene rise of the Bolivian Altiplano: Evidence for removal of mantle lithosphere, *Earth Planet. Sci. Lett.*, *241*, 543–556, doi:10.1016/j.epsl.2005.11.026.

Giacosa, R. (1998), Hoja Geológica 4766-III/IV Puerto Deseado, Provincia de Santa Cruz, scale , 1:250000, Serv. Geol. Minero Argent., Buenos Aires.

Gorring, M. L., and S. M. Kay (2001), Mantle processes and sources of Neogene slab window magmas from southern Patagonia, Argentina, *J. Petrol.*, *42*(6), 1067–1094, doi:10.1093/petrology/42.6.1067.

Gorring, M. L., S. M. Kay, P. K. Zeitler, V. A. Ramos, D. Rubiolo, M. I. Fernandez, and J. L. Panza (1997), Neogene Patagonian plateau lavas: Continental magmas associated with ridge collision at the Chile Triple Junction, *Tectonics*, *16*, 1–17, doi:10.1029/96TC03368.

Gorring, M. L., B. Singer, J. Gowers, and S. M. Kay (2003), Plio-Pleistocene basalts from the Meseta del Lago Buenos Aires, Argentina: Evidence for asthenosphere-lithosphere interactions during slab window magmatism, *Chem. Geol.*, *193*, 215–235, doi:10.1016/S0009-2541(02)00249-8.

Guivel, C., Y. Lagabrielle, J. Bourgois, H. Martin, N. Arnaud, S. Fourcade, J. Cotten, and R. Maury (2003), Very shallow melting of oceanic crust during spreading ridge subduction: Origin of near-trench Quaternary volcanism at the Chile Triple Junction, *J. Geophys. Res.*, *108*(B7), 2345, doi:10.1029/2002JB002119.

Guivel, C., et al. (2006), Miocene to Late Quaternary Patagonian basalts (46–47°S): Geochronometric and geochemical evidence for slab tearing due to active spreading ridge subduction, *J. Volcanol. Geotherm. Res.*, *149*, 346–370, doi:10.1016/j.jvolgeores.2005.09.002.

Gurnis, M. (1993), Phanerozoic marine inundation of continents driven by dynamic topography above subducting slabs, *Nature*, *364*, 589–593, doi:10.1038/364589a0.

Hager, B. H., and R. W. Clayton (1989), Constraints on the structure of mantle convection using seismic observations, flow models and the geoid, in *Mantle Convection*, edited by W. R. Peltier, pp. 657–763, Gordon and Breach, New York.

Haq, B. U., J. Hardenbol, and P. R. Vail (1987), Chronology of fluctuating sea levels since the Triassic (250 millions years ago to present), *Science*, *235*, 1156–1167, doi:10.1126/science.235.4793.1156.

Harper, J. F. (1984), Mantle flow due to internal vertical forces, *Phys. Earth Planet. Inter.*, *36*, 285–290, doi:10.1016/0031-9201(84)90052-9.

Homovc, J. F., G. A. Conforto, P. A. Lafourcade, and L. A. Chelotti (1995), Fold belt in the San Jorge Basin, Argentina: An example of tectonic inversion, in *Basin Inversion*, edited by J. G. Buchanan and P. G. Buchanan, *Geol. Soc. Spec. Publ.*, vol. 88, pp. 235–248.

Husson, L. (2006), Dynamic topography above retreating subduction zones, *Geology*, *34*(9), 741–744, doi:10.1130/G22436.1.

Kay, S. M., V. A. Ramos, and M. Marquez (1993), Evidence in Cerro Pampa volcanic rocks for slab-melting prior to ridge-trench collision in southern South America, *J. Geol.*, *101*, 703–714.

Kraemer, P. E. (1998), Structure of the Patagonian Andes: Regional balanced cross section at 50°S, Argentina, *Int. Geol. Rev.*, *40*, 896–915.

Kraemer, P. E., J. V. Ploszkiewicz, and V. A. Ramos (2002), Estructura de la Cordillera Patagónica Austral entre los 46° y 52°S, provincia de Santa Cruz, Argentina, paper presented at the 15th Congreso Geológico Argentino, Asoc. Geol. Argent., El Calafate, Argentina.

Lagabrielle, Y., M. Suárez, E. A. Rossello, G. Hérail, J. Martinod, M. Régnier, and R. De la Cruz (2004), Neogene to Quaternary evolution of the Patagonian Andes at the latitude of the Chile Triple Junction, *Tectonophysics*, *385*, 211–241, doi:10.1016/j.tecto.2004.04.023.

Lagabrielle, Y., et al. (2007), Pliocene extensional tectonics in the eastern central Patagonian Cordillera: Geochronological constraints and new field evidence, *Terra Nova*, *19*, 413–424, doi:10.1111/j.1365-3121.2007.00766.x.

Lange, D., J. Cembrano, A. Rietbrock, C. Haberland, T. Dahm, and K. Bataille (2008), First seismic record for intra-arc strike-slip tectonics along the Liquiñe-Ofqui fault zone at the obliquely convergent plate margin of the southern Andes, *Tectonophysics*, *455*, 14–24, doi:10.1016/j.tecto.2008.04.014.

Lavenu, A., and J. Cembrano (1999), Compresional- and transpressional-stress pattern for Pliocene and Quaternary brittle deformation in fore arc and intra-arc zones (Andes of central and southern Chile), *J. Struct. Geol.*, *21*, 1669–1691, doi:10.1016/S0191-8141(99)00111-X.

Le Stunff, Y., and Y. Ricard (1997), Partial advection of equidensity surfaces: A solution for the dynamic topography problem?, *J. Geophys. Res.*, *102*, 24,655–24,667, doi:10.1029/97JB02346.

Lock, J., H. Kelsey, K. Furlong, and A. Woolace (2006), Late Neogene and Quaternary landscape evolution of the northern California Coast Ranges: Evidence for Mendocino triple junction tectonics, *Geol. Soc. Am. Bull.*, *118*(9–10), 1232–1246, doi:10.1130/B25885.1.

Lonsdale, P. (2005), Creation of the Cocos and Nazca plates by the fission of the Farallon plate, *Tectonophysics*, *404*, 237–264, doi:10.1016/j.tecto.2005.05.011.

Malumián, N. (1999), La sedimentación y el volcanismo terciarios en la Patagonia extraandina, in *Geología Argentina*, edited by R. Caminos, *Inst. Geol. Recursos Miner. An.*, vol. 29, pp. 557–612.

Marshall, L. G., and P. Salinas (1990), Stratigraphy of the Río Frías Formation (Miocene), along the Alto Río Cisnes, Aisén, Chile, *Rev. Geol. Chile*, *17*, 57–88.

Mercer, J. H. (1976), Glacial history of southernmost South America, *Quat. Res.*, *6*, 125–166, doi:10.1016/0033-5894(76)90047-8.

Mercer, J. H., R. J. Fleck, E. A. Mankinen, and W. Sander (1975), Southern Patagonia: Glacial events between 4 m.y. and 1 m.y. ago, in *Quaternary Studies*, edited by R. P. Guggatre and M. M. Cresswell, pp. 223–230, R. Soc. of N. Z., Wellington.

Mitrovica, J. X., C. Beaumont, and G. T. Jarvis (1989), Tilting of continental interiors by the dynamical effects of subduction, *Tectonics*, *8*, 1079–1094, doi:10.1029/TC008i005p01079.

Mitrovica, J. X., R. N. Pysklywec, C. Beaumont, and A. Rutty (1996), The Devonian to Permian sedimentation of the Russian platform: An example of subduction-controlled long-wavelength tilting of continents, *J. Geodyn.*, *22*(1–2), 79–96, doi:10.1016/0264-3707(96)00008-7.

Molnar, P., P. England, and J. Martinod (1993), Mantle dynamics, uplift of the Tibetan Plateau, and the Indian Monsoon, *Rev. Geophys.*, *31*, 357–396, doi:10.1029/93RG02030.

Morgan, W. (1965), Gravity anomalies and convection currents, *J. Geophys. Res.*, *70*, 6175–6187, doi:10.1029/JZ070i024p06175.

Panza, J. L. (2002), La cubierta detrítica del Cenozoico superior, paper presented at the 15th Congreso Geológico Argentino, Asoc. Geol. Argent., El Calafate, Argentina.

Panza, J. L., and A. Genini (2005), Hoja Geológica 4769-IV Monumento Natural Bosques Petrificados, provincia de Santa Cruz, scale, 1:250,000, Serv. Geol. Minero Argent., Buenos Aires.

Panza, J. L., L. E. Sacomani, and J. C. Cobos (2003), Mapa Geológico de la Provincia de Santa Cruz, República Argentina, scale, 1:750,000, Serv. Geol. Minero Argent., Buenos Aires.

Pardo-Casas, F., and P. Molnar (1987), Relative motion of the Nazca (Farallon) and South American plates since Late Cretaceous time, *Tectonics*, *6*, 233–248, doi:10.1029/TC006i003p00233.

Parras, A., M. Griffin, R. Feldmann, S. Casadío, C. Schweitzer, and S. Marenssi (2008), Correlation of marine beds based on Sr- and Ar-date determinations and faunal affinities across the Paleogene/Neogene boundary in southern Patagonia, Argentina,

J. South Am. Earth Sci., *26*, 204–216, doi:10.1016/j.jsames.2008.03.006.

Peroni, G. O., A. G. Hegedus, J. Cerdan, L. Legarreta, M. A. Uliana, and G. Laffitte (1995), Hydrocarbon accumulation in an inverted segment of the Andean Foreland: San Bernardo Belt, central Patagonia, in *Petroleum Basins of South America*, edited by A. J. Tankard, S. Suárez, and H. J. Welsink, *AAPG Mem.*, vol. 62, pp. 403–419.

Pratt, J. H. (1859), On the deflection of the plumb line in India caused by the attraction of the Himalaya Mountain and of the elevated regions beyond and its modification by the compensation effect of a deficiency of matter below the mountain mass, *Philos. Trans. R. Soc. London*, *149*, 745–778, doi:10.1098/rstl.1859.0029.

Pysklywec, R. N., and J. X. Mitrovica (2000), Mantle flow mechanisms of epeirogeny and their possible role in the evolution of the western Canada Sedimentary Basin, *Can. J. Earth Sci.*, *37*, 1535–1548, doi:10.1139/cjes-37-11-1535.

Ramos, V. A. (1989), Andean foothills structures in northern Magallanes Basin, Argentina, *AAPG Bull.*, *73*(7), 887–903.

Ramos, V. A. (2005), Seismic ridge subduction and topography: Foreland deformation in the Patagonian Andes, *Tectonophysics*, *399*, 73–86, doi:10.1016/j.tecto.2004.12.016.

Ramos, V. A., and S. M. Kay (1992), Southern Patagonian plateau basalts and deformation: Backarc testimony of ridge collisions, *Tectonophysics*, *205*, 261–282, doi:10.1016/0040-1951(92)90430-E.

Ricard, Y., M. Richards, C. Lithgow-Bertelloni, and Y. Le Stunff (1993), A geodynamic model of mantle density heterogeneity, *J. Geophys. Res.*, *98*, 21,895–21,909, doi:10.1029/93JB02216.

Rodriguez, J. F. R., and R. Littke (2001), Petroleum generation and accumulation in the Golfo San Jorge Basin, Argentina: A basin modeling study, *Mar. Pet. Geol.*, *18*, 995–1028, doi:10.1016/S0264-8172(01)00038-1.

Sciutto, J. C., O. Césari, V. Escribano, and H. Pezzuchi (2000), Hoja Geológica 4566-III Comodoro Rivadavia, provincia del Chubut, scale, 1:250,000, Serv. Geol. Minero Argent., Buenos Aires.

Sciutto, J. C., O. Césari, and N. Iantanos (2004), Hoja Geológica 4569-IV Escalante, provincia del Chubut, scale, 1:250,000, Serv. Geol. Minero Argent., Buenos Aires.

Servicio Geológico Minero Argentino (2001), Hoja Geológica 4569-III Sarmiento, provincia del Chubut, scale, 1:250,000, Buenos Aires.

Somoza, R. (1998), Updated Nazca (Farallon)–South America relative motions during the last 40 Ma: Implications for mountain building in the central Andean region, *J. South Am. Earth Sci.*, *11*, 211–215, doi:10.1016/S0895-9811(98)00012-1.

Suárez, M., and R. De la Cruz (2000), Tectonics in the eastern central Patagonian Cordillera plutons, Chile (45°30–47°30′S), *J. Geol. Soc.*, *157*, 995–1001.

Suárez, M., R. De la Cruz, and C. M. Bell (2000), Timing and origin of deformation along the Patagonian fold and thrust belt, *Geol. Mag.*, *137*, 345–353, doi:10.1017/S0016756800004192.

Tassara, A., C. Swain, R. Hackney, and J. Kirby (2007), Elastic thickness structure of South America estimated using wavelets and satellite-derived gravity data, *Earth Planet. Sci. Lett.*, *253*, 17–36, doi:10.1016/j.epsl.2006.10.008.

Thomson, S. N., F. Hervé, and B. Stöckhert (2001), Mesozoic-Cenozoic denudation history of the Patagonian Andes (southern Chile) and its correlation to different subduction processes, *Tectonics*, *20*, 693–711, doi:10.1029/2001TC900013.

Turcotte, D. L., and G. Schubert (1982), *Geodynamics Applications of Continuum Physics to Geological Problems*, John Wiley, New York.

Turner, K. J., C. J. Fogwill, R. D. McCulloch, and D. E. Sugden (2005), Deglaciation of the eastern flank of the North Patagonian Icefield and associated continental-scale lake diversions, *Geogr. Ann.*, *87*, 363–374, doi:10.1111/j.0435-3676.2005.00263.x.

Zhong, S., and M. Gurnis (1994), Controls on trench topography from dynamic models of subducted slabs, *J. Geophys. Res.*, *99*, 15,683–15,695, doi:10.1029/94JB00809.

B. Guillaume, Dipartimento Scienze Geologiche, Università degli Studi Roma TRE, Largo San Leonardo Murialdo 1, I-00146 Roma, Italy. (benjamin.guillaume@uniroma3.it)

L. Husson, Géosciences Rennes, UMR 6118, Université Rennes-1, CNRS, Campus de Beaulieu, F-35042 Rennes CEDEX, France. (laurent.husson@univ-rennes1.fr)

J. Martinod and M. Roddaz, Université de Toulouse, UPS (OMP), LMTG 14, Avenue Édouard Belin, F-31400 Toulouse, France. (martinod@lmtg.obs-mip.fr; mroddaz@lmtg.obs-mip.fr)

R. Riquelme, Departamento de Ciencias Geológicas, Universidad Católica del Norte, Avenida Angamos 0610, Antofagasta, Chile. (rriquelme@ucn.cl)